
Black-box Coreset Variational Inference

Dionysis Manousakas*

Meta[†]

dm754@cantab.ac.uk

Hippolyt Ritter*

Meta

hippolyt@meta.com

Theofanis Karaletsos

Insitro[‡]

theofanis@karaletsos.com

Abstract

Recent advances in coresets methods have shown that a selection of representative datapoints can replace massive volumes of data for Bayesian inference, preserving the relevant statistical information and significantly accelerating subsequent downstream tasks. Existing variational coresets constructions rely on either selecting subsets of the observed datapoints, or jointly performing approximate inference and optimizing pseudodata in the observed space akin to inducing points methods in Gaussian Processes. So far, both approaches are limited by complexities in evaluating their objectives for general purpose models, and require generating samples from a typically intractable posterior over the coresets throughout inference and testing. In this work, we present a black-box variational inference framework for coresets that overcomes these constraints and enables principled application of variational coresets to intractable models, such as Bayesian neural networks. We apply our techniques to supervised learning problems, and compare them with existing approaches in the literature for data summarization and inference.

1 Introduction

Machine learning models are widely trained using mini-batches of data [8, 22], enabling practitioners to leverage large scale data for increasingly accurate models. However, repeatedly processing these accumulating amounts of data becomes more and more hardware-intensive over time and therefore costly. Thus, efficient techniques for extracting and representing the relevant information of a dataset for a given model are urgently needed.

Recent work on coresets for probabilistic models has demonstrated that Bayesian posteriors on large scale datasets can be sparsely represented via surrogate densities defined through a weighted subset of the training data (Sparse Variational Inference; **Sparse VI**) [10] or a set of learnable weighted pseudo-observations in data space (Pseudodata Sparse Variational Inference; **PSVI**) [31]. Similar to inducing points in Gaussian Processes [50], these target to parsimoniously represent the sufficient statistics of the observed dataset that are required for inference in the model. Replacing the original data via the reduced set of (pseudo-) observations unlocks the potential of scaling up downstream learning tasks, compressing for efficient storage and visualisation, and accelerating model exploration.

Unfortunately, Sparse VI and PSVI rely on access to exact samples from the model posterior and closed form gradients of it to be evaluated and updated. Yet, the posterior for most common probabilistic models is intractable, limiting their use to the class of tractable models or necessitating the use of heuristics deviating from the core objective. Dealing with intractable models typically necessitates the use of approximate methods such as variational inference, which has been increasingly popular with the development of black-box techniques for arbitrary models [43].

In this work, we overcome these challenges and introduce a principled framework for performing approximate inference with variational families based on weighted coresets posteriors. This leads

*Equal contribution [†]Now at Amazon [‡]Research supporting this publication done at Meta

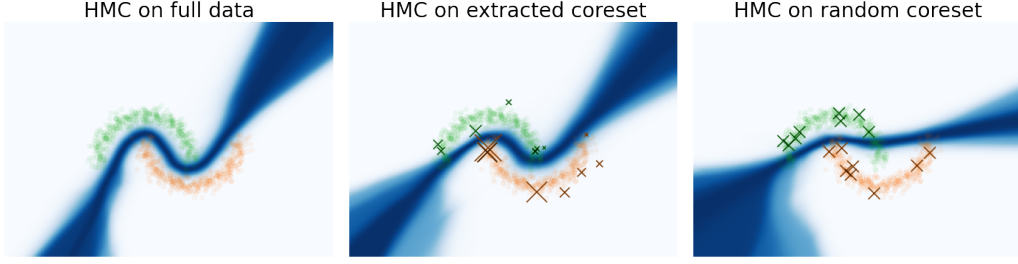


Figure 1: Posterior inference results via Hamiltonian Monte Carlo [35] on the full training dataset, a 16-point coresset learned via BB PSVI, and a 16-point coresset comprised of randomly selected, uniformly weighted data points for half-moon binary classification with a feedforward neural network. Coreset locations are marked in crosses with the size indicating the relative weight. Regions of high predictive uncertainty are visualized by dark blue shaded areas.

to extensions of Sparse VI and PSVI to black-box models, termed **BB Sparse VI** and **BB PSVI**, respectively. As illustrated in Fig. 11 (and further detailed in the supplement) on a synthetic binary classification problem with a Bayesian neural network — an intractable model-class for prior approaches such as PSVI relying on exact posterior samples — BB PSVI is able to learn pseudodata locations and weights inducing a posterior that more faithfully represents the statistical information in the original dataset compared to random selection. However, we emphasize that the utility of coresets goes beyond applying expensive but accurate inference methods to large-scale datasets, and may drive progress in fields such as continual learning as we demonstrate later on.

Specifically, we make the following contributions in this work:

1. We derive a principled interpretation of coresets as rich variational families,
2. we modify the objective to obtain a black-box version of it using importance sampling and a nested variational inference step,
3. utilizing this objective, we propose BB PSVI and BB Sparse VI, two novel suites of variational inference algorithms for black-box probabilistic models,
4. we empirically compare to prior Bayesian and non-Bayesian coresets techniques, and
5. we showcase these techniques on previously infeasible models, Bayesian neural networks.

2 Background

2.1 Variational Inference

Consider a modeling problem where we are given a standard model:

$$p(\mathbf{x}, \mathbf{y}, \boldsymbol{\theta}) = p(\mathbf{y}|\mathbf{x}, \boldsymbol{\theta})p(\boldsymbol{\theta}). \quad (1)$$

Given a dataset $\mathcal{D} = \{(\mathbf{x}, \mathbf{y})\} \subseteq (\mathcal{X} \times \mathcal{Y})^N$, the task of inference and maximization of the marginal likelihood $p(\mathbf{y}|\mathbf{x})$ entails estimation of the posterior distribution over model parameters $\boldsymbol{\theta}$, $p(\boldsymbol{\theta}|\mathbf{x}, \mathbf{y})$. In general, the posterior $p(\boldsymbol{\theta}|\mathbf{x}, \mathbf{y})$ is not tractable. A common solution is to resort to approximate inference, for instance via variational inference (VI). In VI, we assume that we can approximate the true posterior within a *variational family* $q(\boldsymbol{\theta}; \boldsymbol{\lambda})$ with free variational parameters $\boldsymbol{\lambda}$, by minimizing the Kullback-Leibler (KL) divergence between the approximate and the true posterior $D_{\text{KL}}(q(\boldsymbol{\theta}; \boldsymbol{\lambda}) || p(\boldsymbol{\theta}|\mathbf{x}, \mathbf{y}))$, or equivalently by maximizing the Evidence Lower Bound (ELBO):

$$\log p(\mathbf{y}|\mathbf{x}) \geq \text{ELBO}(\boldsymbol{\lambda}) = \mathbb{E}_{q(\boldsymbol{\theta}; \boldsymbol{\lambda})} \left[\log \frac{p(\mathbf{y}|\mathbf{x}, \boldsymbol{\theta})p(\boldsymbol{\theta})}{q(\boldsymbol{\theta}; \boldsymbol{\lambda})} \right]. \quad (2)$$

2.2 (Bayesian) coresets and pseudocoresets

Bayesian coresets constructions aim to provide a highly automated data austere approach to the problem of inference, given a dataset \mathcal{D} and a probabilistic model Eq. (1). Agnostic to the particular

inference method used, Bayesian coresets shrink in a model-specific way the original dataset to a much sparser weighted dataset representation $\{(\mathbf{v}, \mathbf{x}, \mathbf{y})\} \subseteq (\mathbb{R}_{\geq 0} \times \mathcal{X} \times \mathcal{Y})^N$, where $\|\mathbf{v}\|_0 = M \ll N$, that maximizes the parsimony of observations considered over inference, while allowing close approximations of the full data posterior, i.e. $p(\boldsymbol{\theta}|\mathbf{x}, \mathbf{y}, \mathbf{v}) \approx p(\boldsymbol{\theta}|\mathbf{x}, \mathbf{y})$. Initial Bayesian coreset constructions formulated the problem as yielding a sparsity-constrained approximation of the true data likelihood function uniformly over the parameter space. This perspective has admitted solutions via convexifications relying on importance sampling and conditional gradient methods [12, 23], greedy methods for geodesic ascent [11], as well as non-convex approaches employing iterative hard thresholding [56]. Recently, Sparse VI [10] reformulated the problem as performing directly VI within a sparse exponential family of approximate posteriors defined on the coreset datapoints.

PSVI The idea of using a set of learnable weighted *pseudodata* (or *inducing points*) $(\mathbf{v}, \mathbf{u}, \mathbf{z}) := \{(\mathbf{v}_m, \mathbf{u}_m, \mathbf{z}_m)\}_{m=1}^M \subseteq (\mathbb{R}_{\geq 0} \times \mathcal{X} \times \mathcal{Y})^M$ to summarize a dataset for the purpose of posterior inference was introduced in [31], as the following objective:

$$\mathbf{v}^*, \mathbf{u}^*, \mathbf{z}^* = \arg \min_{\mathbf{v}, \mathbf{u}, \mathbf{z}} D_{\text{KL}}(p(\boldsymbol{\theta}|\mathbf{u}, \mathbf{z}, \mathbf{v}) || p(\boldsymbol{\theta}|\mathbf{x}, \mathbf{y})). \quad (3)$$

This objective facilitates learning weighted pseudodata such that the exact posterior of model parameters given pseudodata $p(\boldsymbol{\theta}|\mathbf{u}, \mathbf{z}, \mathbf{v})$ approximates the exact posterior given the true dataset $p(\boldsymbol{\theta}|\mathbf{x}, \mathbf{y})$, and was demonstrated on a variety of models as a generally applicable objective. However, in [31] it was assumed that this objective is tractable, as demonstrated in experiments on models admitting analytical posteriors, or via the use of heuristics to sample from the coreset posterior, as is the case in a logistic regression employing a Laplace approximation.

Sparse VI Sparse VI [10] targets to incrementally minimize the rhs of Eq. (3) via fixing the coreset points locations and optimizing their weights \mathbf{v} . In its original construction, the coreset points are initialized to the empty set and \mathbf{v} to $\mathbf{0}$. In the general case of an intractable model, the coreset posterior is approximately computed via fitting a Laplace approximation $q_{\text{Lap}}(\boldsymbol{\theta}; \mathbf{v})$ on the weighted datapoints of the coreset $(\mathbf{v}, \mathbf{x}, \mathbf{y})$. The next point selection step involves: (i) computing approximations of the centered log-likelihood function of each datapoint (\mathbf{x}_i, y_i) for model parameters $\boldsymbol{\theta}_s$ sampled from the current coreset posterior, via an MC estimate $\tilde{\mathbf{f}}(\mathbf{x}_n, y_n, \boldsymbol{\theta}_s) := \left(\log p(y_n|\mathbf{x}_n, \boldsymbol{\theta}_s) - \frac{1}{S} \sum_{s'=1}^S \log p(y_n|\mathbf{x}_n, \boldsymbol{\theta}_{s'}) \right) \in \mathbb{R}^S$, $\boldsymbol{\theta}_{s'} \sim q_{\text{Lap}}(\boldsymbol{\theta}_{s'}; \mathbf{v})$, (ii) computing correlations with the residual error of the total data log-likelihood $\mathbf{r}(\mathbf{v}) = \mathbf{f}^T(1 - \mathbf{v})$, and (iii) making a greedy selection of the point that maximizes the correlation between the two: $n^* \in \arg \max_{n \in [N]} \begin{cases} |\text{Corr}(\tilde{\mathbf{f}}, \mathbf{r})| & v_n > 0 \\ \text{Corr}(\tilde{\mathbf{f}}, \mathbf{r}) & v_n = 0 \end{cases}$, where $\text{Corr}(\tilde{\mathbf{f}}, \mathbf{r}) := \text{diag} \left[\frac{1}{S} \sum_s \tilde{\mathbf{f}}_s \tilde{\mathbf{f}}_s^T \right]^{-\frac{1}{2}} \left(\frac{1}{S} \sum_s \tilde{\mathbf{f}}_s \mathbf{r}_s^T \right)$. Subsequently, the vector \mathbf{v} gets optimized via minimizing the KL divergence between the coreset and the true posterior. For the variational family of coressets, under the assumption that $\boldsymbol{\theta}$ is sampled from the *true* coreset posterior, the formula of the gradient of the objective in Eq. (3) can be derived, and approximated via resampling from the coreset over the course of \mathbf{v} optimization. At the end of the optimization, the extracted points and weights are given as input to an approximate inference algorithm—commonly a Laplace approximation—which provides the final estimate of the posterior.

3 Black-box coreset Variational Inference

In order to derive a general PSVI objective, we observe that we first need to posit a variational family involving the pseudodata appropriately. Let's assume the (intractable) variational family $q(\boldsymbol{\theta}|\mathbf{u}, \mathbf{z}) := p(\boldsymbol{\theta}|\mathbf{u}, \mathbf{z})$, which has the following particular structure: it is parametrized as the posterior over $\boldsymbol{\theta}$ as estimated given inducing points \mathbf{u}, \mathbf{z} . In this case, $q(\boldsymbol{\theta}|\mathbf{u}, \mathbf{z})$ can be thought of as a *variational program* (see [44]) with variational parameters $\boldsymbol{\phi} = \{\mathbf{u}, \mathbf{z}\}$ and expressed as:

$$q(\boldsymbol{\theta}|\mathbf{u}, \mathbf{z}) := p(\boldsymbol{\theta}|\mathbf{u}, \mathbf{z}) = \frac{p(\mathbf{z}|\mathbf{u}, \boldsymbol{\theta})p(\boldsymbol{\theta})}{p(\mathbf{z}|\mathbf{u})}, \quad (4)$$

where the marginal likelihood term $p(\mathbf{z}|\mathbf{u})$ is typically intractable.

Utilizing this for the formulation of a pseudo-coreset variational inference algorithm leads to the following lower bound on the marginal likelihood of the *true* data:

$$\text{ELBO}_{\text{PSVI}}(\mathbf{u}, \mathbf{z}) = \mathbb{E}_{q(\boldsymbol{\theta}|\mathbf{u}, \mathbf{z})} \left[\log \frac{p(\mathbf{y}|\mathbf{x}, \boldsymbol{\theta})p(\boldsymbol{\theta})}{q(\boldsymbol{\theta}|\mathbf{u}, \mathbf{z})} \right]. \quad (5)$$

Performing VI involves maximizing Eq. (5) with respect to the parameters $\{\mathbf{u}, \mathbf{z}\}$. Scrutinizing this objective reveals that the posterior $q(\boldsymbol{\theta}|\mathbf{u}, \mathbf{z}) := p(\boldsymbol{\theta}|\mathbf{u}, \mathbf{z})$ is used in two locations: **first**, as the *sampling* distribution for $\boldsymbol{\theta}$, **second** to evaluate log-densities of samples (*scoring*). This objective can only be evaluated if the posterior $p(\boldsymbol{\theta}|\mathbf{u}, \mathbf{z})$ can be readily evaluated in closed form and sampled from directly. This causes this expression to remain intractable but for the simplest of cases, and reveals the need to make it computable for any sample $\boldsymbol{\theta}$.

3.1 Bayesian coresets for intractable posteriors

We identified two key problems to evaluate Eq. (5) involving $q(\boldsymbol{\theta}|\mathbf{u}, \mathbf{z})$.

Sampling While we cannot sample from the expectation over $q(\boldsymbol{\theta}|\mathbf{u}, \mathbf{z})$, we can draw K samples from a tractable parametrized distribution $\boldsymbol{\theta}_k \sim r(\boldsymbol{\theta}; \boldsymbol{\psi})$ with variational parameters $\boldsymbol{\psi}$ (i.e. any suitable variational family). However, we cannot plug these samples from r into Eq. (5) directly, as they do not follow the exact distribution called for. To overcome this, we can leverage a self-normalized importance sampling (IS) correction [39] to obtain the desired approximate samples from the coresset posterior. We thus estimate $q(\boldsymbol{\theta}|\mathbf{u}, \mathbf{z})$ via importance sampling by re-weighting samples $\boldsymbol{\theta}$ from the tractable distribution $r(\boldsymbol{\theta}; \boldsymbol{\psi})$. We denote the resulting implicit distribution $q(\boldsymbol{\theta}|\mathbf{u}, \mathbf{z}; \boldsymbol{\psi})$.

We assign the samples *unnormalized* weights w_k :

$$w_k = \frac{p(\mathbf{z}|\mathbf{u}, \boldsymbol{\theta}_k)p(\boldsymbol{\theta}_k)}{r(\boldsymbol{\theta}_k; \boldsymbol{\psi})}, \quad (6)$$

and denote the corresponding *normalized* weights $\tilde{w}_k = w_k / \sum_j w_j$.

Using $q(\boldsymbol{\theta}|\mathbf{u}, \mathbf{z})$ from Eq. (4), we rewrite Eq. (5) as:

$$\begin{aligned} \text{ELBO}_{\text{PSVI-IS}}(\mathbf{u}, \mathbf{z}) &= \int_{\boldsymbol{\theta}} q(\boldsymbol{\theta}|\mathbf{u}, \mathbf{z}) \log \frac{p(\mathbf{y}|\mathbf{x}, \boldsymbol{\theta})p(\boldsymbol{\theta})}{q(\boldsymbol{\theta}|\mathbf{u}, \mathbf{z})} d\boldsymbol{\theta} \\ &= \int_{\boldsymbol{\theta}} \frac{q(\boldsymbol{\theta}|\mathbf{u}, \mathbf{z})}{r(\boldsymbol{\theta}; \boldsymbol{\psi})} r(\boldsymbol{\theta}; \boldsymbol{\psi}) \log \frac{p(\mathbf{y}|\mathbf{x}, \boldsymbol{\theta})p(\boldsymbol{\theta})}{q(\boldsymbol{\theta}|\mathbf{u}, \mathbf{z})} d\boldsymbol{\theta} \approx \sum_{\boldsymbol{\theta}_k \sim r(\boldsymbol{\theta}; \boldsymbol{\psi})} \tilde{w}_k \log \frac{p(\mathbf{y}|\mathbf{x}, \boldsymbol{\theta}_k)p(\boldsymbol{\theta}_k)}{q(\boldsymbol{\theta}_k|\mathbf{u}, \mathbf{z})}. \end{aligned} \quad (7)$$

Scoring After having tackled sampling, we shift our attention to the second problem, evaluating $q(\boldsymbol{\theta}|\mathbf{u}, \mathbf{z})$ inside the logarithm. The key problem with scoring $\log q(\boldsymbol{\theta}|\mathbf{u}, \mathbf{z})$ as defined in Eq. (4) is the intractable marginal probability of the inducing points (IP) $\log p(\mathbf{z}|\mathbf{u})$. We overcome this by introducing a variational approximation to $\log q(\boldsymbol{\theta}|\mathbf{u}, \mathbf{z})$ using the same distribution $r(\boldsymbol{\theta}; \boldsymbol{\psi})$ used above and obtain evidence lower bound ELBO_{IP} of the IP:

$$\log p(\mathbf{z}|\mathbf{u}) \geq \text{ELBO}_{\text{IP}}(\boldsymbol{\psi}) = \mathbb{E}_{r(\boldsymbol{\theta}; \boldsymbol{\psi})} \log \frac{q(\mathbf{z}|\mathbf{u}, \boldsymbol{\theta})p(\boldsymbol{\theta})}{r(\boldsymbol{\theta}; \boldsymbol{\psi})}. \quad (8)$$

Putting it all together We return to Eq. (7) and substitute $q(\boldsymbol{\theta}_k|\mathbf{u}, \mathbf{z})$, per Eq. (4) to derive the following multi-sample importance sampling lower bound on the evidence of the *observed* data and expose the term $\log p(\mathbf{z}|\mathbf{u})$:

$$\text{ELBO}_{\text{PSVI-IS}}(\mathbf{u}, \mathbf{z}) \approx \sum_{\boldsymbol{\theta}_k \sim r} \tilde{w}_k \left[\log \frac{p(\mathbf{y}|\mathbf{x}, \boldsymbol{\theta}_k)p(\mathbf{z}|\mathbf{u})}{p(\mathbf{z}|\mathbf{u}, \boldsymbol{\theta}_k)} \right] = \sum_{\boldsymbol{\theta}_k \sim r} \tilde{w}_k \log \frac{p(\mathbf{y}|\mathbf{x}, \boldsymbol{\theta}_k)}{p(\mathbf{z}|\mathbf{u}, \boldsymbol{\theta}_k)} + \log p(\mathbf{z}|\mathbf{u}).$$

By lower bounding $\log p(\mathbf{z}|\mathbf{u})$ with $\text{ELBO}_{\text{IP}}(\psi)$, we now propose our final black box objective $\text{ELBO}_{\text{PSVI-IS-BB}}$ as a lower bound to $\text{ELBO}_{\text{PSVI-IS}}(\mathbf{u}, \mathbf{z})$, under which we can tractably *score* \mathbf{u}, \mathbf{z} :

$$\begin{aligned} \text{ELBO}_{\text{PSVI-IS}}(\mathbf{u}, \mathbf{z}) &\geq \text{ELBO}_{\text{PSVI-IS-BB}}(\mathbf{u}, \mathbf{z}, \psi) \\ &= \sum_{\theta_k \sim r} \tilde{w}_k \log \frac{p(\mathbf{y}|\mathbf{x}, \theta_k)}{p(\mathbf{z}|\mathbf{u}, \theta_k)} + \mathbb{E}_{\theta \sim r} \left[\log \frac{p(\mathbf{z}|\mathbf{u}, \theta)p(\theta)}{r(\theta; \psi)} \right] \\ &\approx \sum_{\theta_k \sim r} \left[\tilde{w}_k \log \frac{p(\mathbf{y}|\mathbf{x}, \theta_k)}{p(\mathbf{z}|\mathbf{u}, \theta_k)} + \frac{1}{K} \log \frac{p(\mathbf{z}|\mathbf{u}, \theta_k)p(\theta_k)}{r(\theta_k; \psi)} \right]. \end{aligned} \quad (9)$$

We now remind the reader out that by introducing $\text{ELBO}_{\text{PSVI-IS}}$ we lower bounded $\log p(\mathbf{y}|\mathbf{x})$, and that $\text{ELBO}_{\text{PSVI-IS-BB}}$ rigorously lower bounds $\text{ELBO}_{\text{PSVI-IS}}$, showing that our proposed fully tractable black box objective $\text{ELBO}_{\text{PSVI-IS-BB}}$ is a rigorous variational objective for approximating $\log p(\mathbf{y}|\mathbf{x})$:

$$\log p(\mathbf{y}|\mathbf{x}) \geq \text{ELBO}_{\text{PSVI-IS}}(\mathbf{u}, \mathbf{z}) \geq \text{ELBO}_{\text{PSVI-IS-BB}}(\mathbf{u}, \mathbf{z}, \psi).$$

Maximizing $\text{ELBO}_{\text{PSVI-IS-BB}}$ leads to optimizing parameters ψ and thus *adapting* the proposals r for the importance weighting throughout inference, within the confines of the chosen variational family. This is a common approach when blending variational inference and Monte Carlo corrections and can be thought of as specifying an implicit variational family. Depending on the structure of the model one might elect to replace importance sampling with richer Monte Carlo schemes here. We also note that parameters ψ serve maximization of evidence for inducing points given fixed $\{\mathbf{u}, \mathbf{z}\}$, while parameters $\phi = \{\mathbf{u}, \mathbf{z}\}$ are adapted to maximize evidence over observed data $\{\mathbf{x}, \mathbf{y}\}$ which need to account for during optimization of said parameters in Section 3.4. Studying this objective further reveals that replacing our pseudodata dependent importance weights with a uniform distribution $\tilde{w}_k = 1/K$, $k = 1, \dots, K$, or using a single-sample objective (i.e. in the degenerate case when $K = 1$), allows us to recover the classical ELBO of Eq. (2), cancelling the pseudodata likelihood terms in the variational objective.² The setting where we apply this black-box estimator to the basic PSVI algorithm for inferring locations ϕ and model variables ψ will be denoted *BB PSVI*.

3.2 Variational families: (un)weighted inducing points

When studying the objective in Eq. (5) it quickly becomes evident that the exact amount of the selected coresnet datapoints defines the available evidence for that particular posterior construction and as such is a quantity of interest. We will consider this quantity *pseudo-evidence*.

For notational brevity so far we have considered the variational parameters ϕ to represent pseudodata directly, while rescaling using the fixed data compression ratio to maintain invariance of the total pseudo-evidence to the coresnet size. We will be calling this setting *unweighted pseudodata*.

One choice we can make now is to ensure that the available pseudo-evidence is invariant to the chosen size of the coresnet support and potentially equal to the regular dataset. To achieve that, we set:

$$q(\theta|\mathbf{u}, \mathbf{z}) := p(\theta|\mathbf{u}, \mathbf{z}) = \frac{p(\mathbf{z}|\mathbf{u}, \theta)^{N/M} p(\theta)}{p(\mathbf{z}|\mathbf{u})} = \frac{\prod_{i=1}^M p(\mathbf{z}_i|\mathbf{u}_i, \theta)^{N/M} p(\theta)}{p(\mathbf{z}|\mathbf{u})}, \quad (10)$$

with $p(\mathbf{z}|\mathbf{u})$ similarly reweighted via the selected observational *data compression ratio* N/M , i.e. for continuous parameter spaces $p(\mathbf{z}|\mathbf{u}) := \int p(\mathbf{z}|\theta, \mathbf{u})^{N/M} p(\theta) d\theta$.

We may also consider a scenario where we have more generally *weighted pseudodata*, which involves an additional learnable parameter $v_i \geq 0$ per datapoint \mathbf{u}_i and permits the following interpretation: $\mathbf{v}_i \sim \text{Multi}(\mathbf{v})$. Sampling repeatedly from this distribution yields a collection of inducing points with their frequencies governed by their respective weights:

$$q(\theta|\mathbf{v}, \mathbf{u}, \mathbf{z}) := p(\theta|\mathbf{v}, \mathbf{u}, \mathbf{z}) = \frac{p(\theta) \prod_i p(\mathbf{z}_i|\mathbf{u}_i, \theta)^{v_i}}{p(\mathbf{z}|\mathbf{v}, \mathbf{u})}. \quad (11)$$

Simplifying the notation for weighted log-likelihoods throughout, we denote:

$$\log p(\mathbf{z}_i|v_i, \mathbf{u}_i, \theta) := v_i \log p(\mathbf{z}_i|\mathbf{u}_i, \theta). \quad (12)$$

²The nested variational program Eq. (8) still allows propagation of non-zero gradients w.r.t. the pseudodata.

We can now also combine the ideas of learning the weights of pseudodata and controlling the amount of pseudoevidence by posing parametrizations where v_i is non-negative and sums to 1 (e.g. $v_i := \text{softmax}(\beta_i)$, $i = 1, \dots, M$), and adding global variational parameters to optimize the magnitude of total evidence over the pseudodata (e.g. $\log p(z|\mathbf{v}, \mathbf{u}, \boldsymbol{\theta}, \alpha) := \alpha \mathbf{v}^T \log p(z|\mathbf{u}, \boldsymbol{\theta})$), where α can be set by hand (i.e. to N/M) or be an extra learnable quantity. We will explore various such choices for coresnet variational family parametrizations $\phi = \{\mathbf{u}, \mathbf{z}, \mathbf{v}, \alpha\}$ in our experiments and the effects they have on learning.

3.3 Incremental and Batch Black-Box Sparse VI

The estimator we derive can also be used to design a black-box version of the Sparse VI algorithm introduced in [10] (see Sec. 2.2), by the insight that it requires only the variational parameters for coresnet weights to be updated while using copies of real datapoints as coresnet locations. This unlocks various choices to the overall algorithmic flow. The original incremental construction scheme can become black-box via modifying how the approximate posterior on the coresnet data gets computed, and introducing a generalized objective for the optimization of model evidence involving the coresnet parameters. In this construction (*BB Sparse VI*), we posit a variational family $r(\boldsymbol{\theta}; \boldsymbol{\psi})$ (e.g. mean-field variational distributions) and maximize the corresponding ELBO computed on the weighted datapoints of the coresnet. Using the extracted variational approximation, we draw samples from the coresnet and correct for the model. Next, over the greedy selection step, we use the samples and importance weights to compute the centered log-likelihood vectors $\tilde{\mathbf{f}}(\mathbf{x}_n, y_n, \boldsymbol{\theta}_s) := \log p(y_n|\mathbf{x}_n, \boldsymbol{\theta}_s) - \sum_{s'} w_{s'} \log p(y_n|\mathbf{x}_n, \boldsymbol{\theta}_{s'})$, and select the next datapoint via the greedy correlation maximization criterion. Subsequently, to refine the weight vector towards the true data posterior, we maximize w.r.t. $\mathbf{v}, \boldsymbol{\psi}$ an extension of the PSVI ELBO per Eq. (9), where the coresnet data log-likelihood is multiplied by the weight vector \mathbf{v} as in Eq. (12):

$$\text{ELBO}_{\text{Sparse-BBVI}}(\mathbf{v}, \boldsymbol{\psi}) = \sum_{\boldsymbol{\theta}_k \sim r} \left[\tilde{w}_k \log \frac{p(\mathbf{y}|\mathbf{x}, \boldsymbol{\theta}_k)}{p(\mathbf{y}|\mathbf{v}, \mathbf{x}, \boldsymbol{\theta}_k)} + \frac{1}{K} \log \frac{p(\mathbf{y}|\mathbf{v}, \mathbf{x}, \boldsymbol{\theta}_k)p(\boldsymbol{\theta}_k)}{r(\boldsymbol{\theta}_k; \boldsymbol{\psi})} \right]. \quad (13)$$

The importance sampling scheme for the posterior is defined identically to Eq. (6), after substituting the likelihood term with $p(\mathbf{y}|\mathbf{v}, \mathbf{x}, \boldsymbol{\theta}_k)$ for each sample $\boldsymbol{\theta}_k \sim r(\boldsymbol{\theta}_k; \boldsymbol{\psi})$. At each iteration, this variational objective (which, following similar reasoning with the previous section, can be shown to be a lower bound of the evidence), can be maximized wrt the coresnet and variational parameters $\mathbf{v}, \boldsymbol{\psi}$. Moreover, we can omit the incremental inclusion of points to the coresnet, and consider a *batch* version of this construction, where we initialise at a random subset of the original dataset, keep coresnet point locations fixed, and optimize only the weights attached to the coresnet support using Eq. (13) with non-negativity constraints. Finally, we use the variational approximation fit on the coresnet to compute predictive posteriors on unseen datapoints correcting for our importance sampling.

We also define a variant of the algorithm without incremental selection through *pruning* based on the weighting assigned to the coresnet points when optimizing the ELBO of Eq. (13). We can start from a large coresnet size and, after training, reduce the size of the summary by keeping K samples from a multinomial defined on the coresnet points via their so far learned weights, and re-initialising. We provide pseudo-code for the respective methods in Algs. 3–5 in Supplement B.

3.4 Nested optimization

When using a nested optimizer for the maximization of the $\text{ELBO}_{\text{PSVI-IS-BB}}$, rearranging the terms of the objective places our method in the generic cardinality-constrained bilevel optimization framework for data distillation and coresnet constructions [6, 26]. VI maximizing the objective of Eq. (5) inside a parametric family $r(\boldsymbol{\theta}; \boldsymbol{\psi})$ can be reformulated as a bilevel optimization problem as:

$$\mathbf{v}^*, \mathbf{u}^*, \mathbf{z}^* = \arg \min_{\mathbf{v}, \mathbf{u}, \mathbf{z}} L(\mathbf{v}, \mathbf{u}, \mathbf{z}, \boldsymbol{\psi}^*(\mathbf{v}, \mathbf{u}, \mathbf{z}); \mathbf{x}, \mathbf{y}) \quad \text{s.t.} \quad \boldsymbol{\psi}^* = \arg \min_{\boldsymbol{\psi}} \ell(\boldsymbol{\psi}, \mathbf{v}, \mathbf{u}, \mathbf{z}), \quad (14)$$

where

$$L(\mathbf{v}, \mathbf{u}, \mathbf{z}, \boldsymbol{\psi}(\mathbf{v}, \mathbf{u}, \mathbf{z})) = -\text{ELBO}_{\text{PSVI-IS}}(\mathbf{v}, \mathbf{u}, \mathbf{z}, \boldsymbol{\psi}) \quad (15)$$

and

$$\ell(\boldsymbol{\psi}, \mathbf{v}, \mathbf{u}, \mathbf{z}) = -\text{ELBO}(\boldsymbol{\psi}, \mathbf{v}, \mathbf{u}, \mathbf{z}) := -\mathbb{E}_{\boldsymbol{\theta}_k \sim r} \log \frac{p(v_i, \mathbf{z}|\mathbf{u}, \boldsymbol{\theta}_k)p(\boldsymbol{\theta}_k)}{r(\boldsymbol{\theta}_k; \boldsymbol{\psi})}. \quad (16)$$

We optimize via iterative differentiation [29], i.e. trace the gradient computation over the optimization of the variational parameters ψ when solving the inner problem, and use this information at the computation of the outer objective gradient wrt the variational coresets parameters $\phi = \{v, u, z, \alpha\}$.

4 Experiments

In this section we evaluate the performance of our inference framework in intractable models and compare against standard variational inference methods and earlier Bayesian coresets constructions, as well as black-box extensions of existing variational coresets that rely on our generalized ELBO Eq. (9).

As a running baseline with unrestricted access to the training data, we use the standard *mean-field* VI with a diagonal covariance matrix. To capture the implications of enforcing data cardinality constraints, we also construct a *random coresets* using a randomly selected data subset with fixed data locations and fixed likelihood multiplicities correcting for the dataset size reduction, which we then use to optimize a mean-field approximate posterior. As earlier work relied on Laplace approximations on coresets data as a black-box approach for sampling for intractable coresets posteriors, we also experiment with Laplace approximations on random data subsets as an extra baseline. We make code available at www.github.com/facebookresearch/Blackbox-Coresets-VI.

4.1 Logistic regression

First, we perform inference on logistic regression fitting 3 publicly available binary classification datasets [17, 53] with sizes ranging between $10k$ and $150k$ datapoints, and 10 and 128 dimensions. We posit normal priors $\theta \sim \mathcal{N}(0, I)$ and consider mean-field variational approximations with diagonal covariance. In the following, all presented metrics are averaged across 3 independent trials, and we show the means along with the corresponding standard errors.

Impact of variational parameters We present the predictive metrics of accuracy and log-likelihood on the test set in Tables 1 and 2. We observe that coresets methods relying on optimizing pseudodata have the capacity to better approximate inference on the full dataset for small coresets sizes regardless of data dimension, reaching the performance of unrestricted mean-field VI with the use of less than 50 weighted points. In contrast, the approximations that rely on existing datapoints are limited by data dimensionality and need to acquire a larger support to reach the performance of full-data VI (with effects being more evident in `webspam`, which has a data dimensionality of 128). Including variational parameterisations for optimal scaling of the coresets likelihood aids inference, offering faster convergence. Omitting to correct for dataset reduction ($v = 1$) has detrimental effects on predictive performance. As opposed to earlier constructions limited by heuristics on coresets posterior approximation throughout optimization, our variational framework enables approximating the full data posterior within the assumed variational family. Evaluation of predictive metrics and computation time requirements across a wider range of coresets sizes is included in the supplement.

Impact of importance weighting In Fig. 2 we plot the normalized effective sample size (ESS) of our importance weighting scheme for 10 Monte Carlo samples computed on test data. We observe that the posteriors can benefit from IW, achieving non-trivial ESSs, which tend to converge to close values for large coresets sizes. This finding applies at the testing phase also on ablations of the PSVI variational training that replace the IW scheme with uniform sampling.

Importance sampling in high dimensions. Importance sampling can suffer from large variance in high dimensional spaces [39]. Hence, one may be skeptical about the approximation quality the scheme can provide. To this end, in Supplement G we conduct a complementary experiment with a synthetic logistic regression problem. As dimensionality increases, we find that while ESS goes down, it remains non-trivial. More involved sampling methods such as [58] are a promising avenue for leveraging the modular nature of BB PSVI to achieve further performance improvements.

4.2 Bayesian Neural Networks

In this section we present inference results on Bayesian neural networks (BNNs), a model class that previous work on Bayesian coresets did not consider due to the absence of a black-box variational estimator. In the first part we perform inference via black-box PSVI on 2-dimensional synthetic data

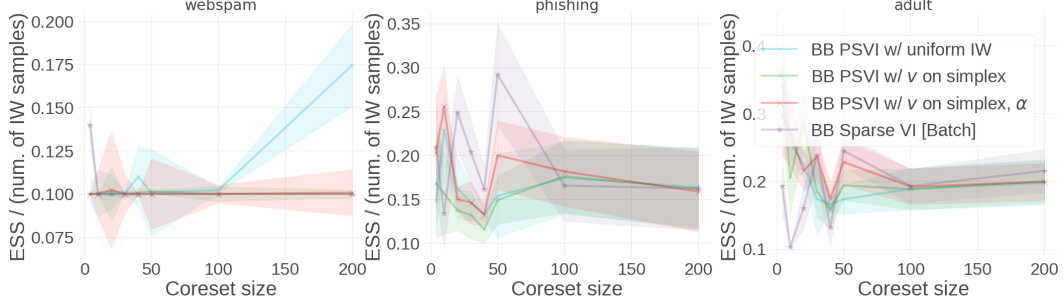


Figure 2: Normalized effective sample size for predictions on test data using 10 Monte Carlo samples from the coresnet posterior over increasing coresnet size.

Table 1: Test accuracy on 3 logistic regression datasets. (*) denotes use of softmax parameterisation for the weights $v = N \text{softmax}(\beta)$.

M	10	webspam			phishing			adult		
		40	100	10	40	100	10	40	100	
BB PSVI	$v(\star), u$	92.2 ± 0.1	92.4 ± 0.1	92.3 ± 0.0	90.1 ± 0.5	91.2 ± 1.0	90.4 ± 0.0	82.2 ± 0.9	83.5 ± 0.2	83.5 ± 0.0
	$v(\star), u, \alpha$	92.2 ± 0.2	92.2 ± 0.1	92.3 ± 0.1	90.7 ± 0.5	90.7 ± 0.9	90.4 ± 0.0	82.6 ± 0.9	83.5 ± 0.0	83.6 ± 0.0
	v, u	92.2 ± 0.1	92.3 ± 0.1	92.2 ± 0.1	90.3 ± 0.8	89.8 ± 0.2	90.3 ± 0.1	80.3 ± 0.8	83.5 ± 0.0	83.5 ± 0.0
	$v = \frac{N}{M} 1, u$	90.9 ± 0.3	91.9 ± 0.1	92.2 ± 0.5	90.2 ± 0.3	88.9 ± 0.7	90.5 ± 0.0	81.0 ± 0.4	83.5 ± 0.1	83.5 ± 0.5
	unif. IW, $v(\star), u$	92.1 ± 0.1	92.3 ± 0.1	92.2 ± 0.1	90.8 ± 1.0	90.6 ± 0.9	90.4 ± 0.0	82.1 ± 0.8	83.5 ± 0.1	83.5 ± 0.0
	w/o IW, $v(\star), u$	90.1 ± 0.6	92.0 ± 0.1	92.3 ± 0.1	90.1 ± 1.4	89.2 ± 1.2	90.4 ± 0.2	77.8 ± 1.5	83.5 ± 0.0	83.5 ± 0.1
	$v=1, u$	61.1 ± 1.8	61.2 ± 4.7	61.2 ± 2.2	85.8 ± 10.4	86.3 ± 11.1	87.3 ± 11.5	75.0 ± 3.7	75.1 ± 1.6	75.8 ± 1.2
	BB Sparse VI	80.1 ± 0.9	86.9 ± 0.2	88.9 ± 0.4	87.6 ± 0.8	90.7 ± 0.3	90.2 ± 1.2	78.1 ± 1.1	82.6 ± 0.4	83.5 ± 0.7
PSVI [31] Sparse VI [10] Subset Laplace Rand. Coreset Full MFVI	Batch	60.7 ± 0.0	76.9 ± 3.3	83.4 ± 4.5	88.8 ± 2.1	88.9 ± 3.7	88.1 ± 2.2	78.6 ± 0.1	81.9 ± 0.9	82.4 ± 0.7
	Incremental	83.9 ± 0.7	88.8 ± 0.4	90.3 ± 0.3	88.3 ± 1.7	89.0 ± 0.9	90.1 ± 0.1	82.5 ± 0.4	83.5 ± 0.0	83.5 ± 0.0
	72.8 ± 3.5	74.2 ± 4.7	74.6 ± 4.8	87.0 ± 1.6	89.3 ± 0.5	90.0 ± 1.4	78.1 ± 2.3	79.0 ± 3.1	80.7 ± 1.9	
	63.0 ± 6.4	78.8 ± 2.3	82.7 ± 1.3	72.7 ± 4.1	84.7 ± 2.1	88.0 ± 2.1	64.4 ± 2.2	77.0 ± 2.2	81.2 ± 1.2	
	71.3 ± 2.9	83.6 ± 1.2	86.3 ± 0.6	81.4 ± 2.7	86.1 ± 3.8	84.4 ± 1.7	75.9 ± 1.1	76.2 ± 0.3	79.5 ± 0.5	
	Full MFVI				92.7 ± 0			90.4 ± 0.1		83.5 ± 0

using single-hidden layer BNNs, while in the latter part we evaluate the performance of our methods on compressing the MNIST dataset using the LeNet architecture [25].

Simulated datasets We generate two synthetic datasets with size $1k$ datapoints, corresponding to noisy samples from a half-moon shaped 2-class dataset, and a mixture of 4 unimodal clusters of data each belonging to a different class [24], and use a layer with 20 and 50 units respectively. To evaluate the representation ability of the pseudocoressets we consider two initialization schemes: we initialise the pseudo locations on a random subset equally split across categories, and a random initialization using a Gaussian centered on the means of the empirical distributions. In Fig. 3 we visualize the inferred predictive posterior entropy, along with coresnet points locations and relative weights. Regardless of the initialization, BB PSVI has the capacity to optimize the locations of the coresnet support according to the statistics of the true data distribution, yielding correct decision boundaries. Importantly, the coresnet support consists itself of separable summarizing pseudo points, while the likelihood reweighting variational parameters enable emphasizing on critical regions of the

Table 2: Test negative log. likelihood on 3 logistic regression datasets.

M	10	webspam			phishing			adult		
		40	100	10	40	100	10	40	100	
BB PSVI	$v(\star), u$	21.7 ± 0.3	21.9 ± 0.2	21.2 ± 0.2	36.1 ± 0.8	34.8 ± 3.8	26.0 ± 0.1	36.1 ± 0.8	34.8 ± 3.8	26.0 ± 0.1
	$v(\star), u, \alpha$	22.1 ± 0.5	21.6 ± 0.2	21.0 ± 0.0	33.6 ± 0.6	34.2 ± 3.1	25.9 ± 0.1	50.2 ± 3.2	34.0 ± 0.0	33.9 ± 0.0
	v, u	21.9 ± 0.4	21.9 ± 0.1	21.6 ± 0.3	40.3 ± 2.1	48.9 ± 6.2	26.0 ± 0.1	78.0 ± 6.2	34.0 ± 0.1	34.0 ± 0.1
	$v = \frac{N}{M} 1, u$	26.4 ± 1.1	23.6 ± 0.3	22.3 ± 1.3	40.8 ± 0.8	57.7 ± 10.9	25.9 ± 0.1	79.5 ± 14.5	33.9 ± 0.1	33.9 ± 1.4
	unif. IW, $v(\star), u$	21.2 ± 0.2	20.8 ± 0.1	31.8 ± 1.8	31.3 ± 2.7	25.9 ± 0.1	48.1 ± 2.2	33.9 ± 0.1	33.9 ± 0.1	
	w/o IW, $v(\star), u$	29.8 ± 2.1	21.8 ± 0.4	21.2 ± 0.3	43.8 ± 5.5	35.8 ± 6.3	26.9 ± 0.5	74.9 ± 10.2	34.2 ± 0.1	34.0 ± 0.3
	$v=1, u$	69.4 ± 3.2	78.4 ± 4.9	70.4 ± 4.7	37.5 ± 24.4	34.7 ± 23.6	38.3 ± 24.8	57.7 ± 7.1	53.1 ± 3.6	49.4 ± 3.0
	BB Sparse VI	65.0 ± 8.6	39.1 ± 1.6	35.9 ± 1.2	40.2 ± 2.9	35.2 ± 0.9	25.9 ± 2.1	70.8 ± 4.4	48.3 ± 1.6	33.9 ± 10.2
PSVI [31] Sparse VI [10] Subset Laplace Rand. Coreset Full MFVI	Batch	86.1 ± 11.0	54.0 ± 3.2	40.7 ± 2.3	33.6 ± 3.6	34.8 ± 3.1	29.4 ± 2.9	45.7 ± 2.2	37.6 ± 1.5	36.5 ± 0.6
	Incremental	81.9 ± 8.4	42.4 ± 0.6	37.2 ± 0.9	32.5 ± 3.1	51.2 ± 16.9	26.0 ± 0.1	40.7 ± 2.4	34.0 ± 0.1	34.0 ± 0.0
	53.9 ± 8.0	52.6 ± 9.3	52.7 ± 9.2	44.0 ± 4.0	38.3 ± 1.9	37.7 ± 2.0	45.3 ± 4.9	44.1 ± 6.1	41.9 ± 4.5	
	96.5 ± 19.0	46.0 ± 3.9	37.8 ± 2.1	55.1 ± 4.7	43.3 ± 4.4	40.9 ± 1.7	119.2 ± 16.3	55.0 ± 9.2	39.4 ± 1.1	
	175.1 ± 25.3	76.9 ± 15.5	83.1 ± 5.8	122.0 ± 13.4	156.0 ± 53.0	47.6 ± 3.4	251.4 ± 32.1	178.5 ± 39.5	51.8 ± 6.7	
	Full MFVI				19.8 ± 0.0			26.1 ± 0.1		33.9 ± 0

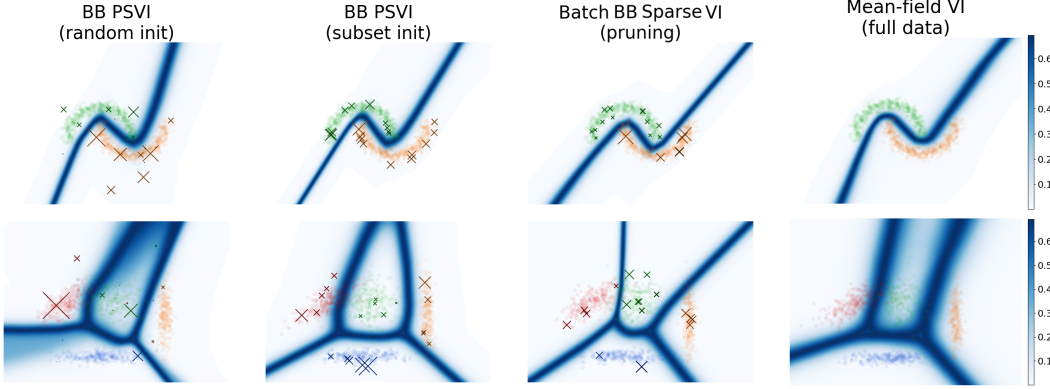


Figure 3: Predictive posterior entropy on simulated datasets. Coreset points are visualised in crosses, with size proportional to their weights.

Table 3: Test accuracy on the MNIST dataset using NNs with the LeNet architecture for our black-box coresnet constructions and other learning baselines. Full MFVI accuracy: 99.13 ± 0.07

	M	10	30	50	80	100	250
BB PSVI	$v(\star), u, z, \alpha$	53.65 \pm 2.48	76.78 \pm 2.1	85.65 \pm 0.0	89.43 \pm 0.56	91.28 \pm 0.74	93.85 \pm 0.0
	$v(\star), u, z$	52.97 \pm 3.32	76.07 \pm 2.06	85.05 \pm 0.3	89.87 \pm 0.95	90.77 \pm 0.92	93.51 \pm 0.14
	$v(\star), u, \alpha$	40.43 \pm 0.66	63.15 \pm 0.14	77.54 \pm 1.32	84.52 \pm 0.18	85.47 \pm 0.21	90.98 \pm 0.33
	$v(\star), u$	40.69 \pm 0.84	62.8 \pm 0.02	76.85 \pm 0.86	84.52 \pm 0.31	86.03 \pm 0.6	91.3 \pm 0.37
BB Sparse VI [Batch]		43.7 \pm 2.14	68.41 \pm 0.6	77.21 \pm 2.43	83.88 \pm 0.44	85.65 \pm 0.17	91.54 \pm 0.16
Dataset Condens. [57]		-	-	-	-	93.9 \pm 0.6	-
SLDD [49]		-	-	-	-	82.7 \pm 2.8	-
Dataset Distill. [54]		-	-	-	-	79.5 \pm 8.1	-
Random Coreset		42.17 \pm 1.74	68.67 \pm 3.21	78.75 \pm 2.17	86.24 \pm 0.25	87.44 \pm 0.32	92.1 \pm 0.65

landscape, assigning larger weights to pseudopoints lying close to the boundaries among the classes. Moreover, our pruning scheme which makes use of batch BB Sparse VI is able to gradually compress a large coresnet of 250 datapoints to a compact performant subset of 20 datapoints arranged in critical locations for learning the Bayesian posterior.

MNIST In this part we assess the approximation quality of large-scale dataset compression for BNNs via coresnets. We compare the predictive performance of black-box PSVI against standard mean-field VI, random coresnets and frequentist methods relying on learnable synthetic data, namely dataset distillation w/ and w/o learnable soft labels [49, 54], and data condensation [57]. We can see that BB PSVI consistently outperforms the random coresnet baseline for coresnet sizes in the orders of few tens or hundreds, however the gap narrows towards 250 coresnet points (Table 3). Moreover, at size 100 our construction provides better test accuracy compared to two frequentist approaches, enjoying the additional advantage of providing uncertainty estimates.

Continual learning with Bayesian coresnets As discussed in the introduction, we envision coresnets being leveraged as a tool beyond scaling sampling methods to large datasets. One such example setting is continual learning, where past methods have encoded statistical information in the form of approximate posterior distributions over the weights [36, 47]. While [36] leverages (randomly selected) coresnets, these necessarily lose information about the data due to the approximate nature of their closed-form posteriors. Bayesian coresnets, in contrast do not make use of an explicit closed-form posterior, as they rely on the implicit posterior induced by the coresnet, representing the prior information by mixing the pseudo data at frequency equal to their weight with the new data. We showcase such a continual learning method on the four-class synthetic problem from above in Fig. 10 with the difference that each class arrives sequentially after the initial two and prior classes are not revisited except for the coresnets (details in Supplement D). Non-Bayesian approaches to continual learning with coresnets have been investigated in more depth in [4, 6, 55].

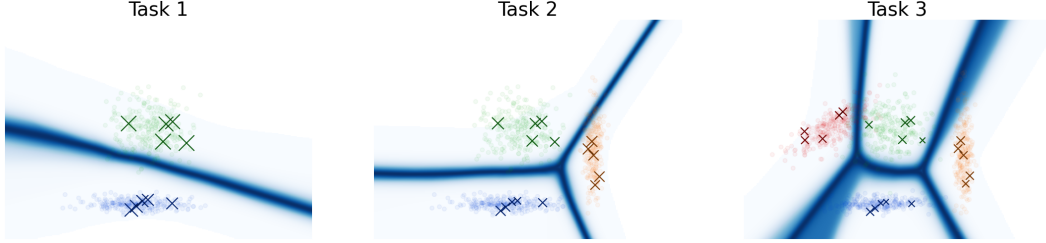


Figure 4: Incremental learning: a coresnet is constructed by incrementally fitting a BNN to 3 classification tasks, starting with 10 coresnet points and subsequently increasing to 15 and 20.

5 Related work and discussion

Coresets and data pruning beyond Bayesian inference The paradigm of coresets emerged from seminal work in computational geometry [1, 18], and has since found broad use in data-intensive machine learning, including least mean square solvers [28], dimensionality reduction [20], clustering [2, 19, 27] and maximum likelihood estimation [3, 32]. Coreset ideas have recently found applications in active learning [42, 7], continual learning [4, 6] and robustness [30, 33]. Recent works in neural networks have investigated heuristics for pruning datasets, including the misclassification events of datapoints over learning [52], or gradient scores in early stages of training [41].

Pseudodata for learning Despite the breakthroughs of classical coresnet methods, the common confine of selecting the coresnets among the constituent datapoints might lead to large summary sizes in practice. Exempt from this limitation are methods that synthesize informative pseudo-examples for training that can summarize statistics lying away from the data manifold. These appear in the literature under various terms, including dataset distillation [26, 29, 54], condensation [57], dataset meta-learning [37] and inducing points [38]. Moreover, recent work [51] has demonstrated that incorporating learnable pseudo-inputs as hyperparameters of the model prior can enhance inference in variational auto-encoders. Learnable pseudodata that resemble the sufficient statistics of the original dataset have also been used in herding [13] and scalable GP inference methods [48, 50].

Variational inference, importance weighting, and Monte Carlo objectives Importance weighting can provide tighter lower bounds of the data log-likelihood for training variational auto-encoders [9], resulting in richer latent representations [14]. In later work, [15] propose an importance weighting VI scheme for general purpose probabilistic inference, while [44, 45] introduce variational programs as programmatic ways to specify a variational distribution. Higher dimensional proposals are commonly handled via Sequential Monte Carlo techniques [16, 34], while [58] develops a family of methods for learning proposals for importance samplers in nested variational approximations. **Two forces** are at play when considering our approximate inference scheme: the variational family r and the sampling scheme used to estimate $q(\theta|u, z; \psi)$. These two interact nontrivially, since r forms the proposal for the importance sampling scheme, and this inference yields gradients for the formation of the coresnet. For hard inference problems richer sampling strategies (e.g. SMC) and variational families may yield useful coresnet and posterior beliefs over the model faster and with more accuracy.

6 Conclusion

We have developed a framework for novel black-box constructions of variational coresnets that can be applied at scale to large datasets as well as richly structured models, and result in effective model-conditional dataset summarization. We overcome the intractability of previous inference algorithms with our proposed black-box objectives, which we develop for both Sparse VI as well as PSVI, and propose a suite of algorithms utilizing them.

Through experiments on intractable models, we show that the inferred coresnets form a useful summary of a dataset with respect to the learning problem at hand, and are capable to efficiently compress information for Bayesian posterior approximations. In future work, we plan to extend this inference toolbox for privacy purposes and non-traditional learning settings, e.g. continual learning, explore alternative objectives, and richer models of coresnets.

References

- [1] P. K. Agarwal, S. Har-Peled, K. R. Varadarajan, et al. Geometric approximation via coresets. *Combinatorial and computational geometry*, 2005.
- [2] O. Bachem, M. Lucic, and A. Krause. Coresets for nonparametric estimation - the case of DP-means. In *ICML*, 2015.
- [3] O. Bachem, M. Lucic, and A. Krause. Practical coresnet constructions for machine learning. *arXiv preprint*, 2017.
- [4] L. Balles, G. Zappella, and C. Archambeau. Gradient-matching coresets for continual learning. *arXiv preprint*, 2021.
- [5] E. Bingham, J. P. Chen, M. Jankowiak, F. Obermeyer, N. Pradhan, T. Karaletsos, R. Singh, P. Szerlip, P. Horsfall, and N. D. Goodman. Pyro: Deep universal probabilistic programming. *JMLR*, 2019.
- [6] Z. Borsos, M. Mutny, and A. Krause. Coresets via bilevel optimization for continual learning and streaming. In *NeurIPS*, 2020.
- [7] Z. Borsos, M. Tagliasacchi, and A. Krause. Semi-supervised batch active learning via bilevel optimization. In *ICASSP*, 2021.
- [8] L. Bottou. Large-scale machine learning with stochastic gradient descent. In *COMPSTAT*. 2010.
- [9] Y. Burda, R. B. Grosse, and R. Salakhutdinov. Importance weighted autoencoders. In *ICLR*, 2016.
- [10] T. Campbell and B. Beronov. Sparse variational inference: Bayesian coresets from scratch. In *NeurIPS*, 2019.
- [11] T. Campbell and T. Broderick. Bayesian coreset construction via greedy iterative geodesic ascent. In *ICML*, 2018.
- [12] T. Campbell and T. Broderick. Automated scalable Bayesian inference via Hilbert coresets. *JMLR*, 2019.
- [13] Y. Chen, M. Welling, and A. J. Smola. Super-samples from kernel herding. In *UAI*, 2010.
- [14] C. Cremer, Q. Morris, and D. Duvenaud. Reinterpreting importance-weighted autoencoders. In *ICLR*, 2017.
- [15] J. Domke and D. R. Sheldon. Importance weighting and variational inference. In *NeurIPS*, 2018.
- [16] A. Doucet, A. M. Johansen, et al. A tutorial on particle filtering and smoothing: Fifteen years later. *Handbook of nonlinear filtering*, 12(656-704):3, 2009.
- [17] D. Dua and C. Graff. UCI Machine Learning Repository. Irvine, CA: University of California. *School of Information and Computer Science*, 2019.
- [18] D. Feldman and M. Langberg. A unified framework for approximating and clustering data. In *STOC*, 2011.
- [19] D. Feldman, M. Faulkner, and A. Krause. Scalable training of mixture models via coresets. In *NeurIPS*, 2011.
- [20] D. Feldman, M. Schmidt, and C. Sohler. Turning big data into tiny data: Constant-size coresets for k-means, PCA, and projective clustering. *SICOMP*, 2020.
- [21] E. Grefenstette, B. Amos, D. Yarats, P. M. Hüt, A. Molchanov, F. Meier, D. Kiela, K. Cho, and S. Chintala. Generalized inner loop meta-learning. *arXiv preprint arXiv:1910.01727*, 2019.
- [22] M. D. Hoffman, D. M. Blei, C. Wang, and J. Paisley. Stochastic variational inference. *JMLR*, 2013.

[23] J. Huggins, T. Campbell, and T. Broderick. Coresets for scalable Bayesian logistic regression. 2016.

[24] S. Kapoor, T. Karaletsos, and T. D. Bui. Variational auto-regressive Gaussian processes for continual learning. In *ICML*, 2021.

[25] Y. LeCun and C. Cortes. MNIST handwritten digit database. 2010. URL <http://yann.lecun.com/exdb/mnist/>.

[26] J. Lorraine, P. Vicol, and D. Duvenaud. Optimizing millions of hyperparameters by implicit differentiation. In *AISTATS*, 2020.

[27] M. Lucic, O. Bachem, and A. Krause. Strong coresets for hard and soft Bregman clustering with applications to exponential family mixtures. In *AISTATS*, 2016.

[28] A. Maalouf, I. Jubran, and D. Feldman. Fast and accurate least-mean-squares solvers. In *NeurIPS*, 2019.

[29] D. Maclaurin, D. Duvenaud, and R. Adams. Gradient-based hyperparameter optimization through reversible learning. In *ICML*, 2015.

[30] D. Manousakas and C. Mascolo. β -Cores: Robust large-scale Bayesian data summarization in the presence of outliers. In *WSDM*, 2021.

[31] D. Manousakas, Z. Xu, C. Mascolo, and T. Campbell. Bayesian pseudocoresets. In *NeurIPS*, 2020.

[32] B. Mirzasoleiman, J. Bilmes, and J. Leskovec. Coresets for data-efficient training of machine learning models. In *ICML*, 2020.

[33] B. Mirzasoleiman, K. Cao, and J. Leskovec. Coresets for robust training of deep neural networks against noisy labels. In *NeurIPS*, 2020.

[34] C. A. Naesseth, F. Lindsten, T. B. Schön, et al. Elements of sequential monte carlo. *Foundations and Trends® in Machine Learning*, 12(3):307–392, 2019.

[35] R. M. Neal. *Bayesian learning for neural networks*. PhD thesis, University of Toronto, 1995.

[36] C. V. Nguyen, Y. Li, T. D. Bui, and R. E. Turner. Variational continual learning. In *ICLR*, 2018.

[37] T. Nguyen, Z. Chen, and J. Lee. Dataset meta-learning from kernel ridge-regression. In *ICLR*, 2021.

[38] T. Nguyen, R. Novak, L. Xiao, and J. Lee. Dataset distillation with infinitely wide convolutional networks. In *NeurIPS*, 2021.

[39] A. B. Owen. *Monte Carlo theory, methods and examples*. 2013.

[40] A. Paszke, S. Gross, S. Chintala, G. Chanan, E. Yang, Z. DeVito, Z. Lin, A. Desmaison, L. Antiga, and A. Lerer. Automatic differentiation in Pytorch. 2017.

[41] M. Paul, S. Ganguli, and G. K. Dziugaite. Deep learning on a data diet: Finding important examples early in training. In *NeurIPS*, 2021.

[42] R. Pinsler, J. Gordon, E. Nalisnick, and J. M. Hernández-Lobato. Bayesian batch active learning as sparse subset approximation. In *NeurIPS*, 2019.

[43] R. Ranganath, S. Gerrish, and D. Blei. Black box variational inference. In *AISTATS*, 2014.

[44] R. Ranganath, D. Tran, J. Altosaar, and D. Blei. Operator variational inference. In *NeurIPS*, 2016.

[45] R. Ranganath, D. Tran, and D. Blei. Hierarchical variational models. In *ICML*, 2016.

[46] H. Ritter and T. Karaletsos. Tyxe: Pyro-based bayesian neural nets for Pytorch. In *MLSys*, 2022.

- [47] H. Ritter, A. Botev, and D. Barber. Online structured Laplace approximations for overcoming catastrophic forgetting. In *NeurIPS*, 2018.
- [48] E. Snelson and Z. Ghahramani. Sparse Gaussian processes using pseudo-inputs. In *NeurIPS*, 2006.
- [49] I. Sucholutsky and M. Schonlau. Soft-label dataset distillation and text dataset distillation. In *IJCNN*, 2021.
- [50] M. Titsias. Variational learning of inducing variables in sparse Gaussian processes. In *AISTATS*, 2009.
- [51] J. Tomczak and M. Welling. VAE with a VampPrior. In *AISTATS*, 2018.
- [52] M. Toneva, A. Sordoni, R. T. des Combes, A. Trischler, Y. Bengio, and G. J. Gordon. An empirical study of example forgetting during deep neural network learning. In *ICLR*, 2019.
- [53] D. Wang, D. Irani, and C. Pu. Evolutionary study of web spam: Webb spam corpus 2011 versus web spam corpus 2006. In *ICCCNAW*, 2012.
- [54] T. Wang, J.-Y. Zhu, A. Torralba, and A. A. Efros. Dataset distillation. *arXiv preprint*, 2018.
- [55] J. Yoon, D. Madaan, E. Yang, and S. J. Hwang. Online coreset selection for rehearsal-based continual learning. In *ICLR*, 2022.
- [56] J. Zhang, R. Khanna, A. Kyrillidis, and S. Koyejo. Bayesian coresets: Revisiting the nonconvex optimization perspective. In *AISTATS*, 2021.
- [57] B. Zhao, K. R. Mopuri, and H. Bilen. Dataset condensation with gradient matching. In *ICLR*, 2021.
- [58] H. Zimmermann, H. Wu, B. Esmaeili, and J.-W. van de Meent. Nested variational inference. In *NeurIPS*, 2021.

A Probabilistic models for classification with learnable soft labels

Including the labels of the pseudodata to the coresets parameters allows more efficient compression, as our summarizing data now live in an expanded space spanning uncertain pseudolabels. In this case we have to adapt our variational objective to capture the divergence between the distribution over the labels corresponding to the soft labeling of the coresets and the predictive distribution under the current variational posterior. This term can be upper bounded per coresset point indexed by m by interpreting the soft labels as categorical probabilities and minimising the KL divergence between the corresponding distribution and the predictive distribution under the approximate posterior as:

$$\begin{aligned}
D_{\text{KL}}(p(y_m | \mathbf{z}_m) || \mathbb{E}_{q(\boldsymbol{\theta})}[p(y_m | \mathbf{u}_m, \boldsymbol{\theta})]) &= \mathbb{E}_{p(y_m | \mathbf{z}_m)} [\log p(y_m | \mathbf{z}_m) - \log \mathbb{E}_{q(\boldsymbol{\theta})}[p(y_m | \mathbf{u}_m, \boldsymbol{\theta})]] \\
&\leq \mathbb{E}_{p(y_m | \mathbf{z}_m)} [\log p(y_m | \mathbf{z}_m) - \mathbb{E}_{q(\boldsymbol{\theta})}[\log p(y_m | \mathbf{u}_m, \boldsymbol{\theta})]] \\
&= \mathbb{E}_{q(\boldsymbol{\theta})} [\mathbb{E}_{p(y_m | \mathbf{z}_m)} [\log p(y_m | \mathbf{z}_m) - \log p(y_m | \mathbf{u}_m, \boldsymbol{\theta})]] \\
&= \mathbb{E}_{q(\boldsymbol{\theta})} [D_{\text{KL}}(p(y_m | \mathbf{z}_m) || p(y_m | \mathbf{u}_m, \boldsymbol{\theta}))], \tag{17}
\end{aligned}$$

where the inequality follows from Jensen's inequality and $-\log$ being convex. In this context y_m is seen as a random variable and not a fixed label value. If the \mathbf{z}_m probabilities are all 1s, corresponding to the fixed label case, this expression reduces to the expected negative log-likelihood of those labels under the approximate posterior and we recover the negative log likelihood part of the classical (negative) ELBO.

B Pseudocode for Sparse VI vs Black-box Sparse VI

For clarity we include an algorithmic description of the incremental version of our black-box scheme for Sparse VI (Algorithm 3), to be contrasted with the earlier construction of [10] which relies on estimates of the analytical gradient of the KL divergence between the coresets and the true posterior (Algorithm 1). The batch version of the black-box Sparse VI construction is presented in Algorithm 4, where the entire support of the coresets gets jointly optimized without a greedy selection step. The corresponding pruning strategy, which is designed to shrink a given coresset size to a coresset with larger sparsity, is described in Algorithm 5. We typically opt for parameterisations of \mathbf{v} that enforce non-negativity (e.g. via the softmax function), hence projection over gradient updates is generally not required.

Algorithm 1 Sparse VI

$\mathbf{v} \leftarrow \mathbf{0} \in \mathbb{R}^M, \mathcal{I} \leftarrow \emptyset$ \triangleright Initialise to the empty coresset
for $k = 1, \dots, K$ **do**
 $(\boldsymbol{\theta})_{s=1}^S \stackrel{\text{i.i.d.}}{\sim} \pi_{\mathbf{v}}$ \triangleright Take S samples from current coresset posterior
 $\mathcal{B} \sim \text{UnifSubset}([N], B)$ \triangleright Obtain a minibatch of B datapoints from the full dataset
 \triangleright Compute likelihood vectors over the coresset and minibatch datapoints for each sample
 $g_s \leftarrow \left(f(x_m, \boldsymbol{\theta}_s) - \frac{1}{S} \sum_{r=1}^S f(x_m, \boldsymbol{\theta}_r) \right)_{m \in \mathcal{I}} \in \mathbb{R}^M$
 $g'_s \leftarrow \left(f(x_b, \boldsymbol{\theta}_s) - \frac{1}{S} \sum_{r=1}^S f(x_b, \boldsymbol{\theta}_r) \right)_{b \in \mathcal{B}} \in \mathbb{R}^B$
 \triangleright Get empirical estimates of correlation over the coresset and minibatch datapoints
 $\widehat{\text{Corr}} \leftarrow \text{diag} \left[\frac{1}{S} \sum_{s=1}^S g_s g_s^T \right]^{-\frac{1}{2}} \left(\frac{1}{S} \sum_{s=1}^S g_s \left(\frac{N}{B} \mathbf{1}^T g'_s - \mathbf{v}^T g_s \right) \right) \in \mathbb{R}^M$
 $\widehat{\text{Corr}}' \leftarrow \text{diag} \left[\frac{1}{S} \sum_{s=1}^S g'_s g'_s^T \right]^{-\frac{1}{2}} \left(\frac{1}{S} \sum_{s=1}^S g'_s \left(\frac{N}{B} \mathbf{1}^T g'_s - \mathbf{v}^T g_s \right) \right) \in \mathbb{R}^B$
 \triangleright Select next point to be attached via max. correlation with the residual error vector
 $n^* \leftarrow \arg \max_{n \in [m] \cup [B]} \left(\left| \widehat{\text{Corr}} \right| \cdot \mathbb{1}[n \in \mathcal{I}] + \widehat{\text{Corr}}' \cdot \mathbb{1}[n \notin \mathcal{I}] \right), \mathcal{I} \leftarrow \mathcal{I} \cup \{n^*\}$
 \triangleright Optimize the weights \mathbf{v} via proj. gradient descent using estimates of the analytical gradient
for $t = 1, \dots, T$ **do**
 $(\boldsymbol{\theta})_{s=1}^S \stackrel{\text{i.i.d.}}{\sim} \pi_{\mathbf{v}}$
 \triangleright Compute likelihood vectors over the coresset and minibatch datapoints for each sample
 $g_s \leftarrow \left(f(x_m, \boldsymbol{\theta}_s) - \frac{1}{S} \sum_{r=1}^S f(x_m, \boldsymbol{\theta}_r) \right)_{m \in \mathcal{I}} \in \mathbb{R}^M$
 $g'_s \leftarrow \left(f(x_b, \boldsymbol{\theta}_s) - \frac{1}{S} \sum_{r=1}^S f(x_b, \boldsymbol{\theta}_r) \right)_{b \in \mathcal{B}} \in \mathbb{R}^B$
 $\hat{\nabla}_{\mathbf{v}} \leftarrow -\frac{1}{S} \sum_{s=1}^S g_s \left(\frac{N}{B} \mathbf{1}^T g'_s - \mathbf{v}^T g_s \right)$ \triangleright Compute MC gradients for variational parameters
 $\mathbf{v} \leftarrow \max(\mathbf{v} - \gamma_t \hat{\nabla}_{\mathbf{v}}, 0)$ \triangleright Take a projected stochastic gradient step
end for
return \mathbf{v}
end for
At test time use $(\boldsymbol{\theta})_{s=1}^S \stackrel{\text{i.i.d.}}{\sim} \pi_{\mathbf{v}}$ to compute the predictive posterior

Algorithm 2 Correction for sampling under coresset

\triangleright Forward inducing and true data through the model using S samples from the coresset variational approximation $\boldsymbol{\theta} \sim r(\boldsymbol{\theta}; \psi)$ and compute $p(\mathbf{y}|\mathbf{x}, \boldsymbol{\theta}) \in \mathbb{R}^{N \times S}, p(\mathbf{z}|\mathbf{v}, \mathbf{u}, \boldsymbol{\theta}) \in \mathbb{R}^{M \times S}$
 \triangleright Compute importance weights for the coresset samples

$$w_s = \log p(\mathbf{z}|\mathbf{u}, \mathbf{v}, \boldsymbol{\theta}_s) - D_{\text{KL}}(r(\boldsymbol{\theta}_s; \psi) || p(\boldsymbol{\theta}_s)), \tilde{w}_s = \frac{w_s}{\sum_{s'} w_{s'}} \text{ for } s = 1, \dots, S.$$

return Importance weights \tilde{w} and correct marginals using

$$\hat{p}(\mathbf{y}|\mathbf{x}) = \tilde{w} p(\mathbf{y}|\mathbf{x}, \boldsymbol{\theta})$$

Algorithm 3 Black-Box Sparse VI [Incremental] (Ours)

$\mathbf{v} \leftarrow \mathbf{0} \in \mathbb{R}^M$, $\mathbf{g} \leftarrow \mathbf{0} \in \mathbb{R}^{S \times M}$, $\mathbf{g}' \leftarrow \mathbf{0} \in \mathbb{R}^{S \times B}$, $\mathcal{I} \leftarrow \emptyset$ \triangleright Initialise to the empty coresset and pick initial ψ for q
for $k = 1, \dots, K$ **do**
 $\mathcal{B} \sim \text{UnifSubset}([N], B)$ \triangleright Obtain a minibatch of B datapoints from the full dataset
 ▷ Optimize wrt ψ on active coresset weighted datapoints with fixed data locations using the classical ELBO
 $(\boldsymbol{\theta})_{s=1}^S \sim r(\boldsymbol{\theta}; \psi)$, $\mathbf{g}_s \in \mathbb{R}^M$, $\mathbf{g}'_s \in \mathbb{R}^B$ \triangleright Forward each datapoint through the statistical model correcting via importance weighting $\tilde{\mathbf{w}}$ to obtain the centered likelihood vectors using a batch S of samples from r (Algorithm 2)
 ▷ Get empirical estimates of correlation over the coresset and minibatch datapoints
 $\widehat{\text{Corr}} \leftarrow \text{diag} \left[\frac{1}{S} \sum_{s=1}^S \mathbf{g}_s \mathbf{g}_s^T \right]^{-\frac{1}{2}} \left(\frac{1}{S} \sum_{s=1}^S \mathbf{g}_s \left(\frac{N}{B} \mathbf{1}^T \mathbf{g}'_s - \mathbf{v}^T \mathbf{g}_s \right) \right) \in \mathbb{R}^M$
 $\widehat{\text{Corr}}' \leftarrow \text{diag} \left[\frac{1}{S} \sum_{s=1}^S \mathbf{g}'_s \mathbf{g}'_s^T \right]^{-\frac{1}{2}} \left(\frac{1}{S} \sum_{s=1}^S \mathbf{g}'_s \left(\frac{N}{B} \mathbf{1}^T \mathbf{g}'_s - \mathbf{v}^T \mathbf{g}_s \right) \right) \in \mathbb{R}^B$
 ▷ Select next point to be attached via max. correlation with the residual error vector
 $n^* \leftarrow \arg \max_{n \in [m] \cup [B]} \left(\left| \widehat{\text{Corr}} \right| \cdot \mathbb{1}[n \in \mathcal{I}] + \left| \widehat{\text{Corr}}' \right| \cdot \mathbb{1}[n \notin \mathcal{I}] \right)$, $\mathcal{I} \leftarrow \mathcal{I} \cup \{n^*\}$
 ▷ Optimize the weights vector \mathbf{v} via projected gradient descent
 for $t = 1, \dots, T$ **do**
 $\mathcal{B} \sim \text{UnifSubset}([N], B)$
 $(\boldsymbol{\theta})_{i=1}^S \sim r(\boldsymbol{\theta}; \psi)$ \triangleright Resample and compute importance weights using Algorithm 2
 ▷ Compute the outer gradient wrt \mathbf{v} using the gradient information of the inner optimization wrt ψ
 $\hat{\nabla}_{\mathbf{v}} \leftarrow \text{autodiff} \left(-\sum_{\boldsymbol{\theta}_i \sim r} \left[\tilde{w}_i \log \frac{p(\mathbf{y}|\mathbf{x}, \boldsymbol{\theta}_i)}{p(\mathbf{y}|\mathbf{v}, \mathbf{x}, \boldsymbol{\theta}_i)} + \frac{1}{S} \log \frac{p(\mathbf{y}|\mathbf{v}, \mathbf{x}, \boldsymbol{\theta}_i)p(\boldsymbol{\theta}_i)}{r(\boldsymbol{\theta}_i; \psi^*)} \right] \right)$
 s.t. $\psi^* = \arg \max_{\psi} \frac{1}{S} \sum_{\boldsymbol{\theta}_i \sim r} \log \frac{p(\psi|\mathbf{v}, \mathbf{x}, \boldsymbol{\theta}_i)p(\boldsymbol{\theta}_i)}{r(\boldsymbol{\theta}_i; \psi)}$
 $\mathbf{v} \leftarrow \max(\mathbf{v} - \gamma_t \hat{\nabla}_{\mathbf{v}}, 0)$ \triangleright Take a projected stochastic gradient step
 end for
 return \mathbf{v}, ψ^*
end for
At test time predict using $r(\boldsymbol{\theta}; \psi^*)$ and correcting via the importance weights $\tilde{\mathbf{w}}$.

Algorithm 4 Black-Box Sparse VI [Batch] (Ours)

$\psi \leftarrow \psi_0$ \triangleright Initialize the variational parameters of the model
 $\mathcal{I} \sim \text{UnifSubset}([N], M)$ \triangleright Get a minibatch of M random indices of datapoints from the data
 $\mathbf{v} \leftarrow \frac{N}{M} \mathbf{1}_{\mathcal{I}}$ \triangleright Assign uniform weights and rescale likelihoods for invariance
for $t = 1, \dots, T$ **do**
 $\mathcal{B} \sim \text{UnifSubset}([N], B)$
 ▷ Use Algorithm 2 to obtain $\boldsymbol{\theta} \sim r(\boldsymbol{\theta}; \psi)$ and the corresponding importance weights $\tilde{\mathbf{w}}$
 ▷ Compute the outer gradient wrt \mathbf{v} using the gradient information of the inner optimization wrt ψ
 $\hat{\nabla}_{\mathbf{v}} \leftarrow \text{autodiff} \left(-\sum_{\boldsymbol{\theta}_i \sim r} \left[\tilde{w}_i \log \frac{p(\mathbf{y}|\mathbf{x}, \boldsymbol{\theta}_i)}{p(\mathbf{y}|\mathbf{v}, \mathbf{x}, \boldsymbol{\theta}_i)} + \frac{1}{S} \log \frac{p(\mathbf{y}|\mathbf{v}, \mathbf{x}, \boldsymbol{\theta}_i)p(\boldsymbol{\theta}_i)}{r(\boldsymbol{\theta}_i; \psi^*)} \right] \right)$
 s.t. $\psi^* = \arg \max_{\psi} \frac{1}{S} \sum_{\boldsymbol{\theta}_i \sim r} \log \frac{p(\psi|\mathbf{v}, \mathbf{x}, \boldsymbol{\theta}_i)p(\boldsymbol{\theta}_i)}{r(\boldsymbol{\theta}_i; \psi)}$
 $\mathbf{v} \leftarrow \max(\mathbf{v} - \gamma_t \hat{\nabla}_{\mathbf{v}}, 0)$ \triangleright Take a projected stochastic gradient step
end for
return \mathbf{v}, ψ^*
At test time predict use $r(\boldsymbol{\theta}; \psi^*)$ and correct via the importance weights $\tilde{\mathbf{w}}$.

Algorithm 5 Black-Box Sparse VI [Batch] Pruning (Ours)

$\mathcal{C} := \{C_1, C_2, \dots\}$ \triangleright Set of coresets sizes in decreasing order for pruning rounds
 $\mathcal{I}_1 \sim \text{UnifSubset}([N], C_1)$ \triangleright Get a minibatch of M random indices of datapoints from the data
 $\mathbf{v} \leftarrow \frac{N}{C_1} \mathbf{1}_{\mathcal{I}}$ \triangleright Initialize to uniform weights and rescale for full-data evidence
for $C_i \in \mathcal{C}$ **do**
 $\mathcal{I} \sim \text{Multi}(\mathbf{v}, C_i)$ \triangleright Initialize the pruned coresset points via C_i samples from current coreset
 $\mathbf{v} \leftarrow \frac{N}{C_i} \mathbf{1}_{\mathcal{I}}$ \triangleright Reinitialize to uniform weights and rescale
 $\psi \leftarrow \psi_0$ \triangleright (Re)initialize the variational parameters of the model
 for $t = 1, \dots, T_i$ **do**
 $\mathcal{B} \sim \text{UnifSubset}([N], B)$
 \triangleright Compute the outer gradient wrt \mathbf{v} using the gradient information of the inner optimization wrt ψ
 $\hat{\nabla}_{\mathbf{v}} \leftarrow \text{autodiff} \left(-\sum_{\theta_i \sim r} \left[\tilde{w}_i \log \frac{p(\mathbf{y}|\mathbf{x}, \theta_i)}{p(\mathbf{y}|\mathbf{v}, \mathbf{x}, \theta_i)} + \frac{1}{S} \log \frac{p(\mathbf{y}|\mathbf{v}, \mathbf{x}, \theta_i)p(\theta_i)}{r(\theta_i; \psi^*)} \right] \right)$
 s.t. $\psi^* = \arg \max_{\psi} \frac{1}{S} \sum_{\theta_i \sim r} \log \frac{p(\psi|\mathbf{v}, \mathbf{x}, \theta_i)p(\theta_i)}{r(\theta_i; \psi)}$
 $\mathbf{v} \leftarrow \max(\mathbf{v} - \gamma_t \hat{\nabla}_{\mathbf{v}}, 0)$ \triangleright Take a projected stochastic gradient step
 end for
 return \mathbf{v}, ψ^*
end for
At test time predict using $r(\theta; \psi^*)$ and correcting via the importance weights $\tilde{\mathbf{w}}$.

Table 4: Dataset statistics and hyperparameters for batch coresets used throughout experimental results of Section 4.

Dataset	D	N _{tr}	N _{te}	ψ	initial learning rate					σ_{ψ_0}	Inner iters	Batch size
					u	v	α	z				
webspam	128	100,948	25,237	10^{-3}	10^{-4}	10^{-3}	10^{-3}	-	10^{-6}	100	256	
phishing	11	8,844	2,210	10^{-3}	10^{-3}	10^{-3}	10^{-3}	-	10^{-6}	100	256	
adult	11	24,130	6,032	10^{-3}	10^{-4}	10^{-3}	10^{-3}	-	10^{-6}	100	256	
half-moon	2	800	200	10^{-4}	10^{-2}	10^{-1}	10^{-3}	-	10^{-4}	50	128	
four-class	2	800	200	10^{-4}	10^{-2}	10^{-1}	10^{-3}	-	10^{-3}	50	128	
MNIST	(1, 28, 28)	60,000	10,000	10^{-3}	10^{-2}	10^{-2}	10^{-3}	10^{-2}	10^{-10}	20	256	

Table 5: Hyperparameters for incremental coresets used throughout experimental results of Section 4.

Dataset	ψ	initial learning rate					Inner iters	Outer iters	Batch size	MC samples
		ψ_{Laplace}	$v_{\text{Sparse VI}}$	$v_{\text{BB Sparse VI}}$	σ_{ψ_0}					
webspam	10^{-3}	10^{-1}	10^{-1}	10^{-1}	10^{-3}	200	400	512	64	
phishing	10^{-1}	10^{-1}	10^{-2}	10^{-2}	10^{-6}	50	200	256	64	
adult	10^{-1}	10^{-1}	10^{-2}	10^{-2}	10^{-6}	50	200	256	32	

C Experiments details

In this section we provide additional details for our experimental setup, and further evaluation including experimentation over extended coreset size ranges, time plots and preliminary results with hypergradients as an alternative to iterative differentiation for bilevel optimization.

Note that to compute expectations under the intractable true posterior for prediction on the test data using samples from the learned coreset posterior, assuming $q(\boldsymbol{\theta}|\mathbf{u}, \mathbf{z}; \psi) \approx p(\boldsymbol{\theta}|\mathbf{x}, \mathbf{y})$, we can sample from r and correct again using the importance sampling scheme as follows:

$$\mathbb{E}_{p(\boldsymbol{\theta}|\mathbf{x}, \mathbf{y})}[f(\boldsymbol{\theta})] = \int f(\boldsymbol{\theta})p(\boldsymbol{\theta}|\mathbf{x}, \mathbf{y})d\boldsymbol{\theta} \approx \int f(\boldsymbol{\theta}) \frac{q(\boldsymbol{\theta}|\mathbf{u}, \mathbf{z})}{r(\boldsymbol{\theta}; \psi)} r(\boldsymbol{\theta}; \psi) d\boldsymbol{\theta} \approx \sum_{\boldsymbol{\theta}_i \sim r(\boldsymbol{\theta}; \psi)} \tilde{w}_i f(\boldsymbol{\theta}_i). \quad (18)$$

$$\mathbb{E}_{q(\boldsymbol{\theta}|\mathbf{x}, \mathbf{y})}[f(\boldsymbol{\theta})] \approx \sum_{\boldsymbol{\theta}_i \sim r(\boldsymbol{\theta}; \psi)} \tilde{w}_i f(\boldsymbol{\theta}_i). \quad (19)$$

C.1 Hyperparameters

For the experiments on batch coresets and baselines within the family of mean-field variational approximations presented in Section 4, we report the optimal mean predictive accuracy achieved, over independent runs of inference trials, with learning rates for model and coreset parameters taking values from 10^{-4} to 10^{-1} over logarithmic scale. We summarize dataset statistics, corresponding learning rates, along with the remaining selected hyperparameters (namely initialization of variance of our variational approximation, length of inner optimization loop and mini-batch size) for batch constructions of this set of experiments in Table 4. At our estimators we used 10 Monte Carlo samples from the coreset posteriors.

For incremental coresets we tuned the learning rates of the coreset weights v to higher values: given that coreset evidence is initialised to 0 in Algorithms 1 and 3, we found empirically that, via allowing faster growth on the magnitude of the weight vector, the coreset construction can more easily escape local minima in the small size regime. Moreover, we allowed larger numbers of Monte Carlo samples: apart from being involved in the gradient estimation, in incremental coreset constructions this quantity defines the dimension of the geometry used at the greedy next point selection step, hence affording more samples can allow better selection of the coreset support. Larger learning rates on coreset parameters imply reduced stability over training iterations and a higher difficulty in hyperparameter tuning, hence demonstrate in practice the benefits attained by parameterisations that control the

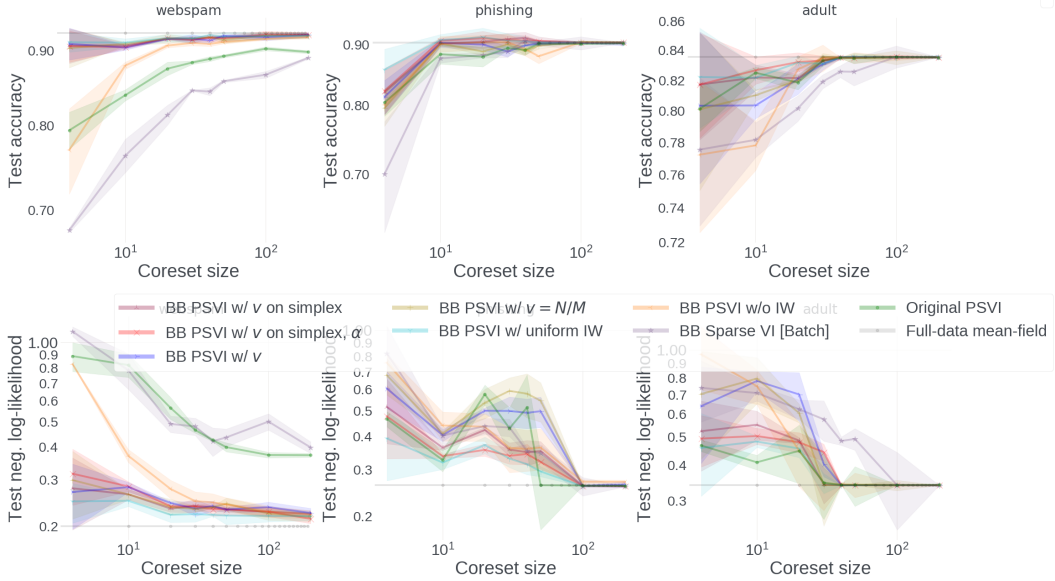


Figure 5: Predictive metrics across longer trials for the logistic regression experiment.

coreset evidence (see Section 3.2). We detail the choices for presented results in Table 5. We denote by ψ_{Laplace} the learning rate used for fitting Laplace approximation on the logistic regression model (as done in the Sparse VI construction), as opposed to ψ which is used when fitting a variational model on the coresset data (as done in BB Sparse VI); we also differentiate by indexing the learning rates for weights for the two Sparse VI constructions.

For the subset Laplace baseline we ran 500 gradient updates of a Laplace approximation with diagonal covariance, and used the Adam optimizer with learning rate 10^{-2} , minibatches of size 256 and 32 Monte Carlo samples.

For Batch BB Sparse VI pruning we reset optimizers, and reinitialise the model and coresset parameters upon application of each pruning step. For the BNN experiment on the synthetic dataset we successively reduced in rounds from 250 initial datapoints to 100 and finally 20 datapoints, allowing training for 200 outer gradient updates before applying each pruning step.

In our bilevel problem, both for the nested and for the outer optimization, we use the Adam optimizer with the default hyperparameter setting of PyTorch implementation [40] and learning rates initialized per Table 4. For iterative differentiation we used the `higher` library [21]. For HMC we use the Pyro [5] implementation through TyXe [46]. Unless otherwise stated these hyperparameter choices will be followed in the additional experiments of this part. In this section, the labels of the pseudocoreset datapoints are always kept fixed.

C.2 Computational resources

The entire set of experiments was executed on internal CPU and GPU clusters. For the logistic regression experiment, we used CPUs allocating two cores with a total of 20GB memory per inference method, while for the Bayesian neural networks we assigned each coresset trial to a single NVIDIA V100 32GB GPU.

C.3 Logistic regression

Predictive metrics In Fig. 5 we present the predictive metrics we obtained across our full trials spanning coresset sizes from 4 to 200 on the 3 logistic regression datasets considered in Section 4.1. We note that for the incremental coressets we do not have direct control on the exact range of constructed coresset sizes over the experiment: At each trial we allocate a maximum number of next point selection steps for these methods, which however acts only as an upper bound of the attained largest coresset size (as an existing point might be reselected multiple times over the greedy

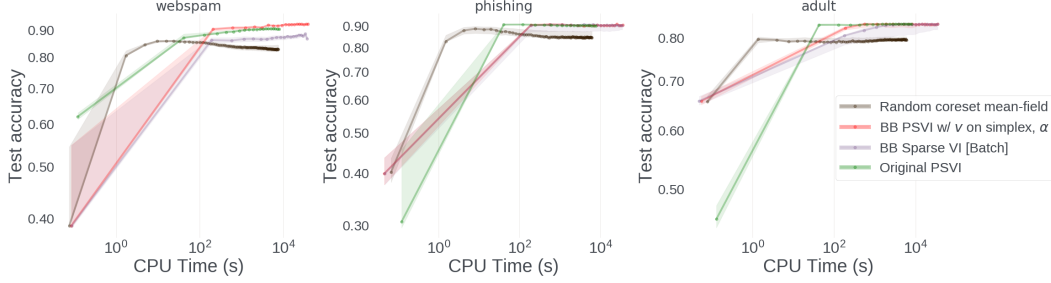


Figure 6: Test accuracy vs CPU time requirements with coresnet size 100 for variational inference using a random coresnet, PSVI, BB PSVI and BB Sparse VI Batch constructions at the logistic regression experiment.

next point addition steps). Indeed, for the Sparse VI construction [10] the coresets did not grow beyond 100 datapoints over the course of the experiment, and we did not include this method in the evaluation of this section. Moreover, for ease of visualization we removed baselines resulting in high variance, including the random coresnet and BB-PSVI w/o rescaling. We can notice that the black-box constructions are capable to converge to the unconstrained mean-field posterior for sufficient coresnet size, while convergence of the original PSVI construction might be limited by the heuristics employed over gradient computation (see `webspam` plot). Moreover, pseudocoreset methods achieve better approximation quality for small coresnet size in high dimensions compared to Sparse VI and other true points selection methods.

Computation time requirements In Fig. 6 we contrast the CPU time requirements for the execution of BB PSVI, BB Sparse VI, PSVI and the random coresnet with $M = 100$ on our experiment, under usage of the same computational resources. Both pseudocoreset approaches solve a bilevel optimization problem, employing though starkly different machinery: BB PSVI relies on nested variational inference, while PSVI requires drawing samples from the true coresnet posterior which are then used in estimating the analytical expression for the objective gradient. Hence, in the general case Monte Carlo sampling is required for asymptotically exact computation at every outer gradient step for PSVI, which makes it more expensive compared to our black-box construction. In practice a Laplace fit is used to approximate the coresnet posterior; hence, making similar assumptions on the expressiveness of the coresnet posterior (mean-field variational family vs Laplace with diagonal covariance), practical implementations of PSVI share the same order of time complexity with BB PSVI. However, BB PSVI is able to reach a higher peak (corresponding to the full data approximation of the selected variational family), as optimization is not hindered by amendments for intractability in the gradient expression. Finally, the gradient computation for BB PSVI via iterative differentiation—which was the optimizer of choice in this experiment—generally implies a higher memory footprint, as tracing the gradient of the inner optimization is required; this requirement can be alleviated via switching from a nested iterative differentiation optimizer to one that makes use of hypergradient approximations (see also next subsection).

C.4 Bayesian Neural Networks

Dynamics over the course of inference In Figs. 7 and 8 we present more instances extracted from the same experimental setting that was demonstrated at convergence (bottom rows) in Figure 3 of Section 4. We can discern the different dynamics in the optimization of pseudodata locations across our proposed constructions and initializations: Initialized on random noise, BB PSVI dynamics at the first stages separate the inducing points according to their categories; next, the inducing points are placed along the decision boundary, and more weight is assigned on data lying on critical locations of the empirical distributions corresponding to the different classes. Initialized on a random subset of the true data, BB PSVI convergence gets accelerated as the first two phases of move are not required. In the case of Batch BB Sparse VI, the locations of the coresnet support are fixed, and gradually the scheme adjusts the weights to the importance of the data, prunes away the ones contributing redundant statistical information, and focuses on keeping data lying on the ends of the class distributions, that jointly specify the decision boundaries. Figure 9 demonstrates the evolution of our black-box

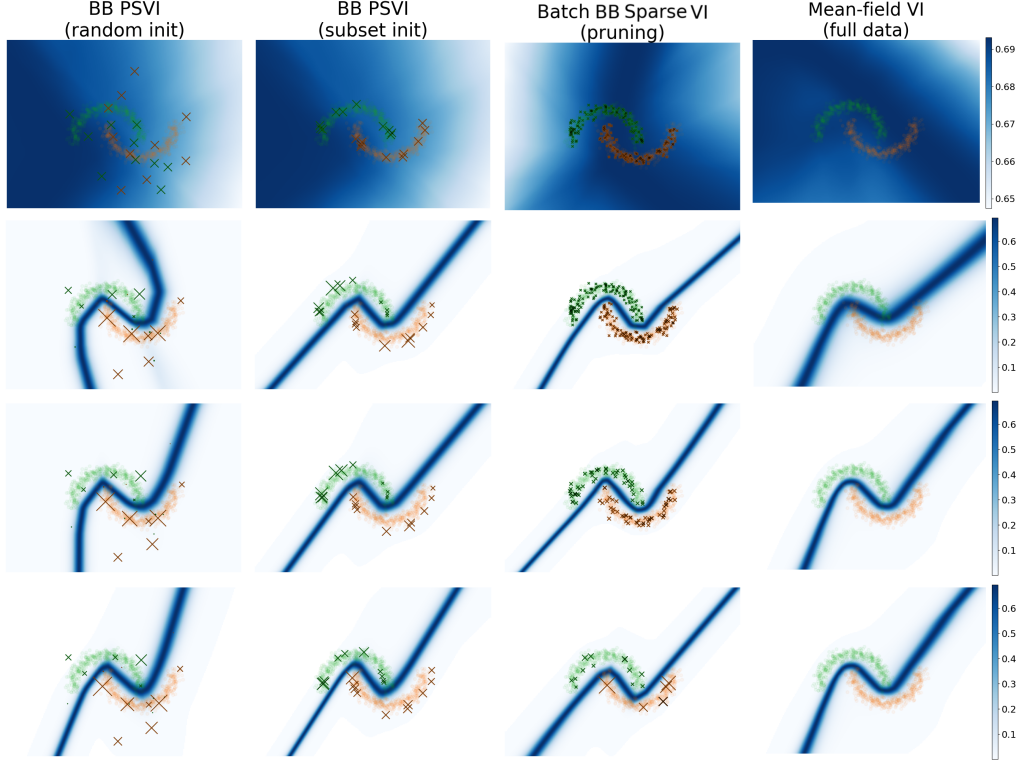


Figure 7: The different dynamics of coresset data optimization at four equidistant instances across the iterations of our inference trial for BB PSVI with 20 points sampled from a Gaussian, BB PSVI with initialization on a random subset of size 20, and Batch BB Sparse VI inducing sparsity via stepwise pruning $M = 250 \rightarrow 100 \rightarrow 20$ points. Mean-field VI on full-data is also plotted for reference.

variational objective for the coressets over a single trial. We notice that the objective presents more variance in the first stages of inference for random initialisation, as the noisy datapoints have to move significantly to discriminate the classes, however it can quickly reach the curve corresponding to the subset initialisation. Regarding BB Sparse VI with pruning, we observe that, despite reinitializations of the network and the coresset point weights, the selection of good summarizing datapoints allows an overall increase of the variational objective, coping with the enforced shrinkage of the coresset size, and eventually achieving similar bounds with the coressets that use variational data.

Justification of pruning strategy Considering the interpretation of weights on the coresset datapoints as probabilities of a multinomial distribution that is learned on the data throughout inference in a way that preserves approximate Bayesian posterior computations (Section 3.2), allows us to justify our pruning step, where a larger coresset gets replaced by K samples from this distribution. In this sense, pruning can be thought of as a means to introduce sparsity while minimizing diverging from the full-data posterior, as this operation corresponds to getting a small number of samples from the learned multinomial on the data, and retraining the model constrained on this sample.

D Continual learning

In Fig. 10 we apply black-box PSVI in a more challenging learning setting defined on the four class dataset, similarly to the synthetic data classification experiment presented in [24] for continually learning inducing points for Gaussian processes—a closely related concept to coressets. Instead of seeing training data from all 4 classes at once, we start with a 2-class classification problem, and, over 2 learning stages, the 3rd and 4th class get sequentially revealed. Whenever we move to the next classification problem, we:

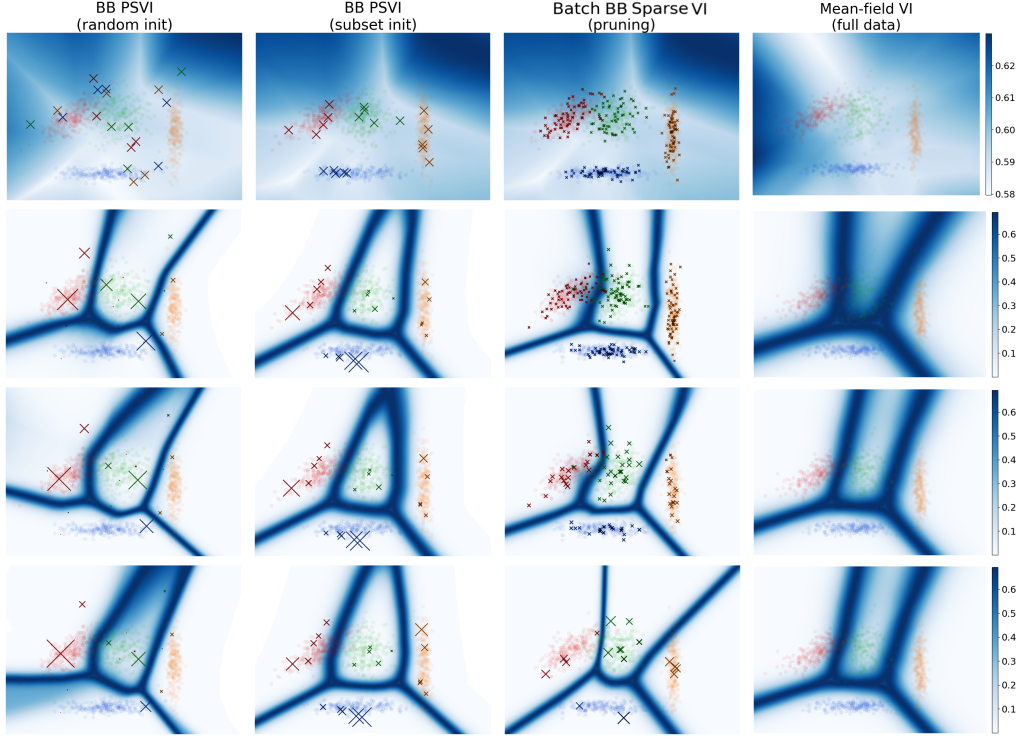


Figure 8: Counterpart of Fig. 7 with four snapshots over training for the multi-class dataset.

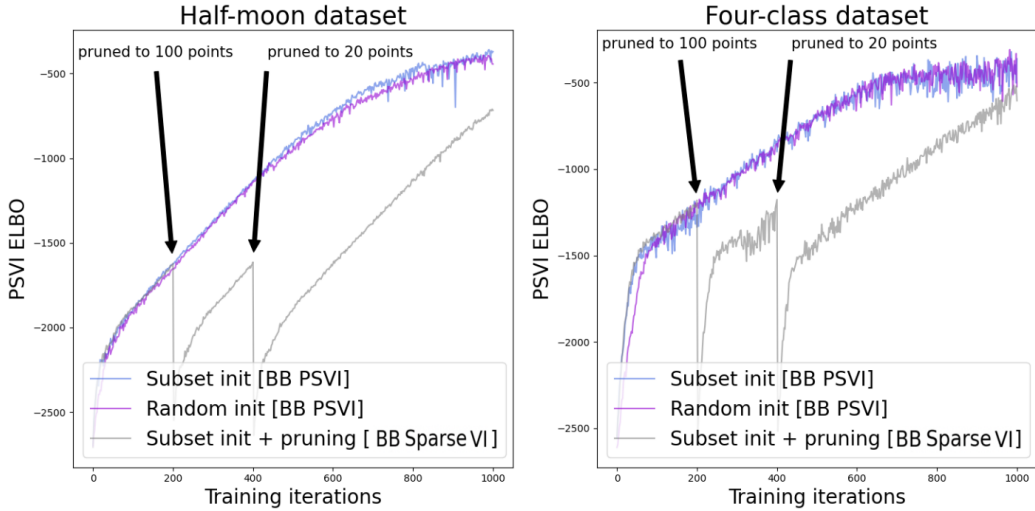


Figure 9: Variational objective vs outer gradient updates for the considered constructions of PSVI and Batch BB Sparse VI with pruning on the synthetic datasets. BB PSVI optimizes a batch of 20 pseudopoints since the beginning of training, while BB Sparse VI starts with a summary of 250 existing datapoints and gradually shrinks it to a batch of 20 informative datapoints after two rounds of pruning and retraining.

- remove all N_k true training data seen so far, and instead use N_k samples *only* from the coresset support according to a multinomial defined via the vector \mathbf{v} of coresset point weights,
- augment the coresset support with a new set of learnable datapoints from the most recently added class, initialising them at a total evidence proportional to the class size, and

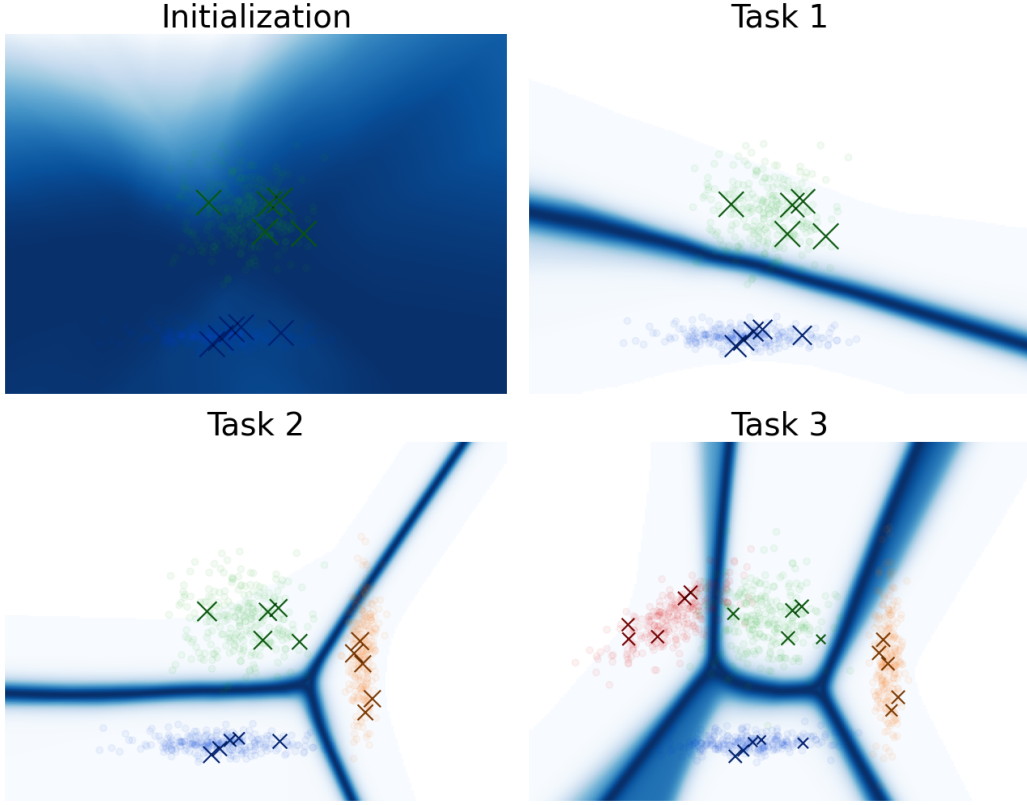


Figure 10: Continual learning setting: A coresset is constructed so that a BNN is fitted incrementally to the 3 classification tasks. We start with a coresset comprised of 10 points and over tasks 2 and 3 we increase coresset size to 15 and 20 datapoints respectively.

- reinitialise all variational parameters ψ and adapt the last layer of our architecture to the number of classes of the new learning stage.

We can notice that the BB PSVI construction is able to successfully represent the historical training data, addressing the common issue of catastrophic forgetting, and provide representative posteriors throughout the 3 stages of our continual learning setting. Even though designed to summarise statistics of earlier tasks, the coresset point locations and weights can be readapted to each new learning task, keeping the essential statistical information from the past.

E Monte Carlo inference on coresets

Extending on the introductory figure from the main text, in Fig. 11 we assess the results of running MCMC inference on the extracted variational coressets for a feedforward BNN trained on the halfmoon data. We visualise 100,000 samples using Hamiltonian Monte Carlo after a warmup period of 20,000 samples. We can notice that the variational coresset using BB PSVI is able to perform more intelligent selection of inducing point locations and weights, e.g. via placing increased importance on the ends of the halfmoon manifolds, hence being able to represent the original training dataset more compactly. This is reflected in an approximate posterior that is closer to the corresponding posterior computed on the full data; in contrast, random subsampling is prone to variance and often misses information about critical regions of the decision boundary. Overall, accelerating MCMC inference without losing much statistical information, as achieved via BB PSVI, can lead to better modeling of uncertainty on large scale data, compared to applying a fully variational treatment.

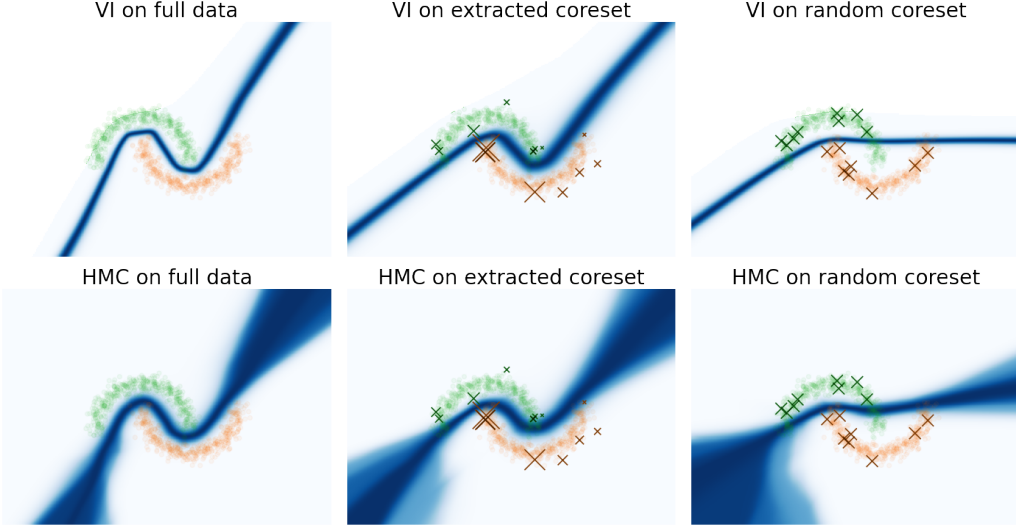


Figure 11: Posterior inference results via variational inference and Hamiltonian Monte Carlo on the full training dataset, a 16-points coresset learned via black-box PSVI, and a 16-points coresset comprised of uniform weights and datapoints selected uniformly at random. All inference methods use the halfmoon dataset and the same probabilistic model based on a feedforward BNN.

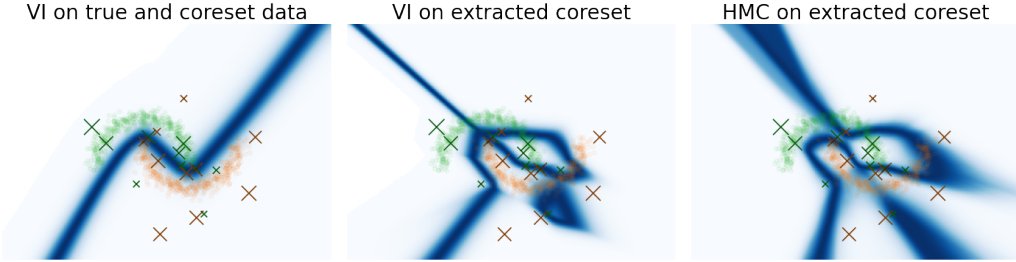


Figure 12: Effects of joint optimization on coresset posterior, using a feedforward BNN and a coresset with 20 datapoints on the halfmoon dataset. Blue shades represent predictive uncertainty, circles the original training data and crosses the coresset point locations with size proportional to the corresponding inferred weight.

F Joint optimization of coresset support and variational parameters

In Fig. 12 we visualize the effects of jointly learning optimized coresset points locations and weights, along with variational parameters using the $\text{ELBO}_{\text{PSVI-IS-BB}}$ from Eq. (9). If we do not constrain the learning of variational parameters to the coresset points, these are unable to distill the relevant information from the true training data for our statistical model. As the joint optimization might be primarily driven by the true data, the coresset support might end up in non-representative locations of the data space, potentially resulting in incorrect decision boundaries after removing the original training datapoints as exhibited in this experiment. The design choices for HMC in this experiment are identical to Fig. 11.

G Importance sampling vs data dimensionality

In Fig. 13 we visualise the normalized effective sample size (ESS) using 10 Monte Carlo samples from our approximate posterior evaluated on the test data throughout PSVI inference. ESS takes consistently non-trivial values (larger than 0.1) even for 200-dimensional data, with a visible decreasing trend as data—and hence model—parameters dimensionality increases. Similarly to [12], the synthetic data for this experiment were generated using covariates $x_n \in \mathbb{R}^d$ sampled i.i.d. from $\mathcal{N}(0, I)$, and binary labels generated from the logistic likelihood with parameter $\theta = 5 \cdot \mathbf{1}_d$. We

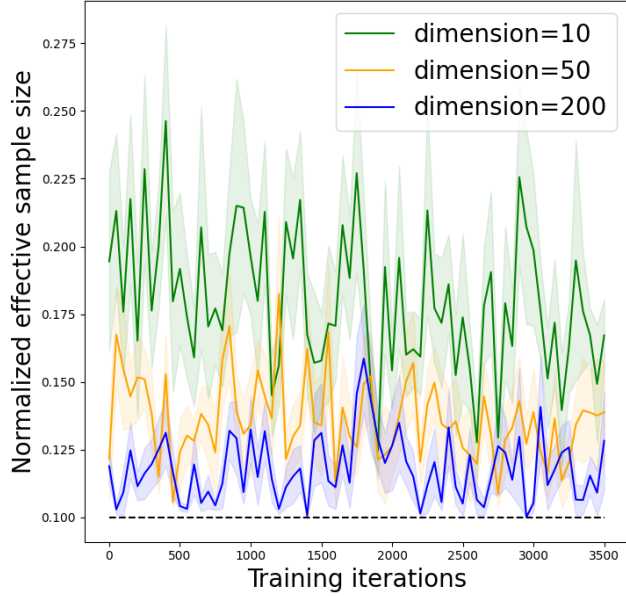


Figure 13: Normalized effective sample size (with standard errors) vs data dimensionality for inference using PSVI with 10 Monte Carlo samples in the Bayesian logistic regression model.

generated a total of $N = 1,000$ datapoints, with 20% of them used as test data, and constructed coressets of size $M = 20$.

H Visualization of MNIST summarizing data

In Fig. 14 we display the learned images and soft-labels for the coresets of size 30 constructed as part of the MNIST compression experiment. We can notice that the basic features of the original images are preserved in the pseudo-images, while the soft labels mainly assign larger score to the class of the corresponding image, and capture the uncertainty between similarly looking classes (e.g. 6 vs 8).

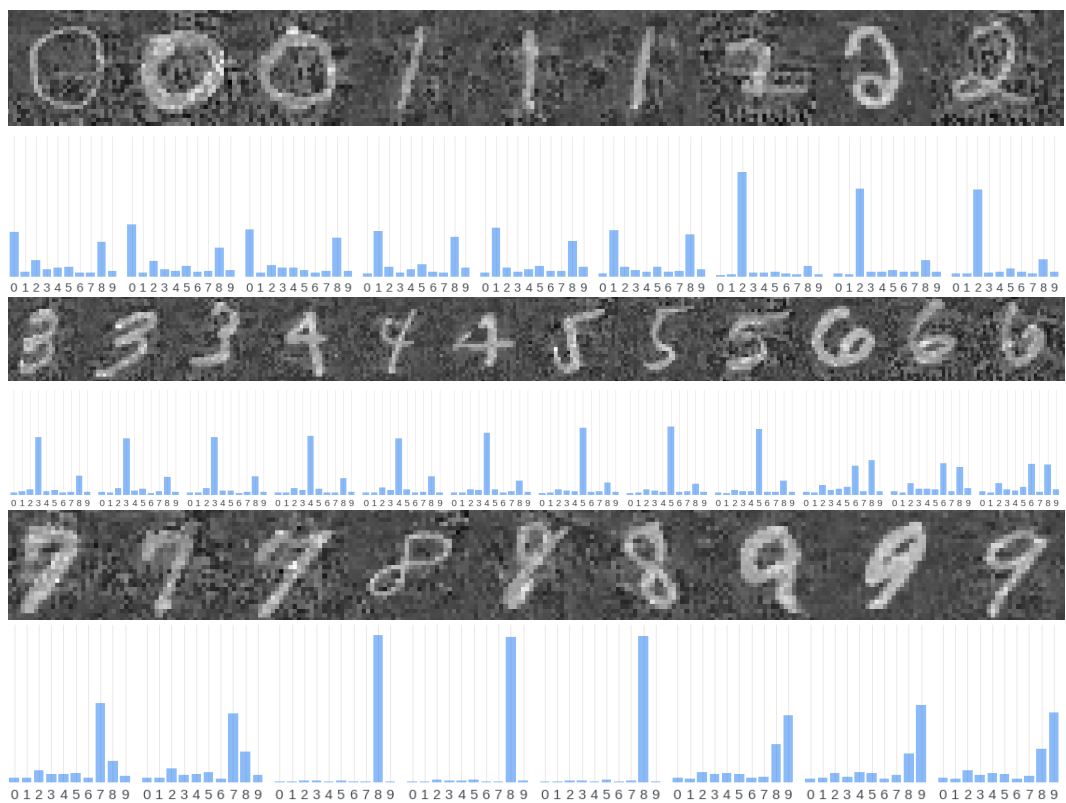


Figure 14: Visualization of the images and corresponding soft-labels for 30 pseudodata learned via black-box PSVI in the MNIST summarization experiment.